# Characteristic function pricing with the Heston-LIBOR hybrid model

**Christopher Sterley**
**Supervised by: Tom McWalter**

A dissertation submitted to the Faculty of Commerce, University of Cape Town, in partial fulfilment of the requirements for the degree of Master of Philosophy.

August 29, 2019

*MPhil in Mathematical Finance,*
*University of Cape Town.*

# Declaration

I declare that this dissertation is my own, unaided work. It is being submitted for the Degree of Master of Philosophy to the University of Cape Town. It has not before been submitted for any degree or examination.

Signed by candidate

Chris Sterley

August 29, 2019

# Abstract

We derive an approximate characteristic function for a simplified version of the Heston-LIBOR model, which assumes a constant instantaneous volatility structure in the underlying LIBOR market model. We also implement measures to improve the numerical stability of the characteristic function derived in this dissertation as well as the one derived by Grzelak and Oosterlee. The ultimate aim of the dissertation is to prevent these characteristic functions from exploding for given parameter values.

# Contents

# List of Figures

# List of Tables

# Chapter 1

# Introduction

The pricing of contingent claims has become more sophisticated since the introduction of Black-Scholes pricing techniques. As is often the case in modelling, when attempting to model a scenario, one usually starts by making simplifying assumptions. This was the case for Black and Scholes who, amongst other assumptions, assumed that market interest rates and asset volatilities were constant. These assumptions have been shown not to be appropriate in application, and their use results in prices of contingent claims that do not reflect important market characteristics.

Heston (1993) extended the Black-Scholes model to allow for stochastic volatility in the asset process: a highly desirable characteristic. Heston (1993) was able to show that, if one were to assume a particular class of dynamics for the asset variance process, then it is possible to determine a closed-form characteristic function for the asset process that can be used with Fourier pricing techniques for an efficient calibration process. This set of dynamics could then be combined with Monte Carlo simulation techniques to determine prices for more exotic contingent claims.

The next logical step is to include stochastic interest rates into the asset dynamics so as to give the potential for an even more realistic characterisation of a market. Grzelak and Oosterlee (2011) initially augmented Heston asset dynamics to allow for stochastic interest rates. This augmentation resulted in the Heston model with a stochastic interest rate process specified by the Hull-White or CIR processes (Hull and White, 1996), (Cox *et al.*, 1985).

However, it is the LIBOR Market Model (LMM) that has become the benchmark interest rate model in practice. Thus, its inclusion as the model which drives the interest rate portion of a hybrid model would allow for the eventual market model to better match market practice. So, instead, Grzelak and Oosterlee (2012) modelled

the interest rate component of the asset dynamics using a set of LMM dynamics. They made use of the variant of LMM proposed by Piterbarg (2005), which allowed for stochastic volatility as well as the interest rate smile to be captured by the final model. This combination of Heston (1993) and Piterbarg (2005) resulted in the H-LMM hybrid model.

However, this hybrid combination results in the total number of components of the model increasing drastically, compared to a hybridisation using a short-rate model. This means that the process of calibrating the model becomes cumbersome, even when using the proposed a-priori calibration of the LMM. As a result, Grzelak and Oosterlee (2012) sought to determine a characteristic function for this hybrid model. Their focus was applying the techniques presented in Duffie *et al.* (2000), as it allows for a characteristic function to be implied by solving a system of ODEs. However, this technique requires that the model is affine in its state space. This is generally not the case, and Grzelak and Oosterlee (2012) linearised the non-affine terms in order to be able to apply the result in Duffie *et al.* (2000). These linearised approximations came at the expense of an adjustment to the Kolmogorov kernel which means that the new approximate model, called the H1-LMM, does not necessarily guarantee the no-arbitrage condition.

Whilst Grzelak and Oosterlee (2012) were able to determine an approximate characteristic function for the hybrid model, it can be shown that this characteristic function is not numerically stable for a range of parameter values. As a result, some remedy is required to improve the stability of the characteristic function, due to the potential benefit that it would be able to provide.

In addition to improving the numerical instability of the resulting characteristic function presented by Grzelak and Oosterlee (2012), a characteristic function is also derived for a Heston-LMM hybrid model, except the LMM model dynamics will have constant instantaneous volatility. A note is provided on how to include deterministic instantaneous volatility in the characteristic function. This allows market practitioners who elect to use the deterministic or constant instantaneous volatility LMM to also make use of this hybrid model, without needing to calibrate a new interest rate model.

The first part of this derivation mirrors that of Grzelak and Oosterlee (2012), however when applying the result in Duffie *et al.* (2000) the derivation begins to deviate. Despite this initial deviation, the resulting characteristic function is anal-

ogous with that of Grzelak and Oosterlee (2012), and also suffers from a similar numerical instability. Thus, this characteristic function is also adjusted in order to improve numerical stability.

The first section of this dissertation will present the dynamics that the equity and interest rate processes in the constant volatility hybrid model are based on. This is followed by a derivation of the characteristic function of the constant instantaneous volatility LMM version of the Hybrid model. The results from this characteristic function, as well as a replication of the characteristic function results presented in Grzelak and Oosterlee (2012) are presented. Finally, characteristic function adjustments are explored, and the results of the subsequent adjustments are presented.

# Chapter 2

# Deriving an Equity-Interest Rate Hybrid Model with Deterministic Interest Rate Volatility

## 2.1 The Underlying Equity and Interest Rate Processes of the Hybrid Model

### 2.1.1 Heston Model Dynamics

Heston (1993) proposed the following system of dynamics for equity processes:

$$\frac{dS_t}{S_t} = r(t)dt + \sqrt{\epsilon_t}dW_x(t), \qquad S_0 > 0, \tag{2.1}$$

$$d\epsilon_t = \kappa(\bar{\epsilon} - \epsilon_t)dt + \gamma\sqrt{\epsilon_t}dW_\epsilon(t), \qquad \epsilon_0 > 0, \tag{2.2}$$

where $S_t$ is the asset price process, $\epsilon_t$ is the asset variance process, $r(t)$ is the risk-free rate, and $W_x(t)$ and $W_\epsilon(t)$ are the Brownian motions, under the risk-neutral measure, for the asset and the variance processes respectively. All other terms are constants. $\epsilon_t$ is a mean-reverting process, with $\bar{\epsilon}$ being the mean-reversion level and $\kappa$ being the rate of mean reversion. The correlation between the asset price process and its variance process is $\rho_{x,\epsilon}$. Note that, in this case, $r(t)$ is a deterministic function of time. We will look to extend the model to allow for this interest rate process to be driven by a stochastic process instead.

### 2.1.2 Interest Rate Model Dynamics

We now look at the dynamics for the interest rate process that we are going to use to model the risk-free rate in the above Heston model. We will be presenting the LMM with deterministic volatility. For a given set of tenors $\mathcal{T} = \{T_0, T_1, \ldots, T_N\}$,

with accrual periods $s_k = T_k - T_{k-1}$, for $k = 1, \ldots, N$, define $B(t, T_i)$ to be the price of a zero-coupon bond (ZCB) at time $t$, which matures at time $T_i$, and has a face value of one unit of currency. Observe that we define $T_{-1} := 0$. Further define the forward LIBOR rate as $F_t^k := F(t; T_{k-1}, T_k)$, where:

$$F(t; T_{k-1}, T_k) \equiv \frac{1}{s_k}\Big(\frac{P(t, T_{k-1})}{P(t, T_k)} - 1\Big) \text{ for } t < T_{k-1}. \tag{2.3}$$

Define $\mathbb{Q}^{T_i}$ to be the measure that uses the $B(t, T_i)$ ZCB as a numeraire. As suggested by Brigo and Mercurio (2007), under this measure, the dynamics for the LIBOR rates is specified by the following system of SDE's:

$$\begin{aligned}
&i < k, t \leq T_i\text{: } dF_t^k = \sigma_k(t)F_t^k \sum_{j=i+1}^{k} \frac{\rho_{k,j} s_j \sigma_j(t) F_t^j}{1 + s_j F_t^j} dt + \sigma_k(t) F_t^k dW_k(t),\\
&i = k, t \leq T_{k-1}\text{: } dF_t^k = \sigma_k(t)F_t^k dW_k(t),\\
&i > k, t \leq T_{k-1}\text{: } dF_t^k = -\sigma_k(t)F_t^k \sum_{j=k+1}^{i} \frac{\rho_{k,j} s_j \sigma_j(t) F_t^j}{1 + s_j F_t^j} dt + \sigma_k(t) F_t^k dW_k(t),
\end{aligned} \tag{2.4}$$

where $\sigma_k(t)$ is the instantaneous volatility function of the $k^{th}$ LIBOR rate and $\rho_{i,j}$ is the correlation between the $i^{th}$ and $j^{th}$ LIBOR rate.

As was pointed out by Grzelak and Oosterlee (2012), given the nature of Equity option pricing, it would be more convenient to work under the $T_N$-measure i.e. the measure associated with the last observable ZCB, $B(t, T_N)$. Under this measure, the LIBOR dynamics for the $k^{th}$ LIBOR rate is given by (2.4). Observe here that $\sum_{i=N+1}^{N} = 0$, such that the $N^{th}$ LIBOR rate is a martingale. Moreover, we take $dW_i^N(t) dW_j^N(t) = \rho_{i,j} dt$.

Using this definition of the LIBOR rate in (2.3), we can define ZCB prices in terms of LIBOR rates through the following equality:

$$B(t, T_k) = \frac{B(t, T_{m(t)})}{\prod_{j=m(t)+1}^{k} (1 + F_j(t, T_{j-1}, T_j))}, \tag{2.5}$$

where $m(t) = \min(k : t < T_k)$. The short-dated ZCB, $B(t, T_{m(t)})$, is not well-defined in the above LIBOR framework. Some interpolation scheme will need to be used in order to determine its price. Some schemes are proposed by Grzelak and Oosterlee (2012).

## 2.2 The Hybrid Model

In this section, we focus on specifying the hybrid model. However, before moving on to specification, it is useful to determine the price of a European call option under the $T_N$-measure given that this is the measure we will be working under throughout.

Observe that we can write the price of a European call option (under the $T_N$-measure) as:

$$\begin{aligned} C(t) &= P(t)\mathbb{E}^{\mathbb{Q}}\Big[\frac{1}{P(T_N)}(S_{T_N}-K)^+|\mathcal{F}_t\Big] \\ &= B(t,T_N)\mathbb{E}^{T_N}\Big[\frac{(S_{T_N}-K)^+}{B(T_N,T_N)}|\mathcal{F}_t\Big] \\ &= B(t,T_N)\mathbb{E}^{T_N}\Big[(Z^{T_N}-K)^+|\mathcal{F}_t\Big], \end{aligned}$$

where

$$Z^{T_N}(t) := \frac{S_t}{B(t,T_N)}, \tag{2.6}$$

and $P(t)$ is the numeraire associated with the risk-neutral measure. This is the reason why we use the LMM dynamics associated with the terminal measure. As we will be pricing vanilla options under this measure, using an interest rate process associated with this measure will ensure that our discounted assets are all martingales.

### 2.2.1 Deriving the Hybrid Model

Now that we have specified the equity and interest rate processes, we can move on to using these in deriving the hybrid model. Note that the bulk of the proof in this section comes from Grzelak and Oosterlee (2012). Given that, under the $T_N$-measure, we require the forward price in order to determine the call price, it is clear that we need to determine the dynamics of the forward rate process.

Thus, it would be useful to define the Heston dynamics specifically under the $T_N$-measure. We assume that, under the $T_N$-measure, the asset and asset variance process have the following dynamics:

$$\begin{aligned} \frac{dS_t}{S_t} &= (\dots)dt + \sqrt{\epsilon_t}dW_x^N(t), \\ d\epsilon_t &= \kappa(\bar{\epsilon}-\epsilon_t)dt + \gamma\sqrt{\epsilon_t}dW_\epsilon^N(t). \end{aligned} \tag{2.7}$$

Observe that we are working with an asset that is discounted by $B(t,T_N)$ i.e. a martingale under the $T_N$-measure. This means that the final dynamics will not have any $dt$ terms, so that specifying the drift term of the asset process is not necessary.

We will be using a correlation structure between the asset price process, the asset variance process, and the interest rate process as follows:

$$dW_x^N(t)dW_\epsilon^N(t) = \rho_{x,\epsilon}dt, \tag{2.8}$$
$$dW_x^N(t)dW_j^N(t) = \rho_{x,j}dt, \tag{2.9}$$
$$dW_i^N(t)dW_j^N(t) = \rho_{i,j}dt, \tag{2.10}$$
$$dW_i^N(t)dW_\epsilon^N(t) = 0. \tag{2.11}$$

In other words, we will be assuming that the asset variance process is independent of all the LIBOR rates. This assumption is consistent with Grzelak and Oosterlee (2012), and has been included in order to maintain consistency with their result.

We now use these dynamics and those specified in (2.4) to determine the forward price dynamics. Applying Ito's formula to $Z^{T_N}(t)$, defined in (2.6), we get:

$$\begin{aligned}
dZ^{T_N}(t) &= \frac{1}{B(t,T_N)}dS_t + S_t d\Big(\frac{1}{B(t,T_N)}\Big) + d\Big[S_t, \frac{1}{B(t,T_N)}\Big], \\
&= \frac{1}{B(t,T_N)}dS_t - \frac{S_t}{B^2(t,T_N)}dB(t,T_N) + \frac{S_t}{B^3(t,T_N)}(dB(t,T_N))^2 \\
&\quad - \frac{1}{B^2(t,T_N)}dS_t dB(t,T_N), \\
&= (\dots)dt + \frac{1}{B(t,T_N)}dS_t - \frac{S_t}{B(t,T_N)^2}dB(t,T_N), \\
&= (\dots)dt + Z^{T_N}(t)\sqrt{\epsilon_t}dW_x^N(t) - \frac{Z^{T_N}(t)}{B(t,T_N)}dB(t,T_N).
\end{aligned} \tag{2.12}$$

Where the second last line follows from the fact that $Z^{T_N}(t)$ is a martingale under the $T_N$-measure, and the last line follows by substituting in (2.7) and from the definition of $Z^{T_N}(t)$.

It is clear from (2.12) that we require the ZCB dynamics under the $T_N$-measure in order to proceed. First, substitute $B(t,T_{m(t)}) = (1+(T_{m(t)}-t)F_{m(t)}(T_{m(t)}))^{-1}$ into (2.5). This allows us to write:

$$B(t,T_N) = (1+(T_{m(t)}-t)F_{T_{m(t)}}^{m(t)})^{-1} \prod_{j=m(t)+1}^{N}(1+\tau_j F_t^j)^{-1}, \tag{2.13}$$

Taking logs in the above equation allows us to re-write (2.13) as:

$$\begin{aligned}\log B(t,T_N) &= -\log(1+(T_{m(t)}-t)F^{m(t)}_{T_{m(t)}}) - \sum_{j=m(t)+1}^{N}\log(1+\tau_j F^j_t),\\ \implies d\log B(t,T_N) &= -d\log(1+(T_{m(t)}-t)F^{m(t)}_{T_{m(t)}})\\ &\quad - \sum_{j=m(t)+1}^{N} d\log(1+\tau_j F^j_t). \end{aligned} \tag{2.14}$$

On the other hand we also have the following relationship by Ito's formula:

$$d\log B(t,T_N) = \frac{1}{B(t,T_N)}dB(t,T_N) - \frac{1}{2}\Big(\frac{1}{B(t,T_N)}\Big)(dB(t,T_N))^2. \tag{2.15}$$

As noted above, we are not concerned with any $dt$ terms. Thus, after dropping these $dt$ terms and setting equations (2.14) and (2.15) equal to eachother, we get the following:

$$\frac{dB(t,T_N)}{B(t,T_N)} = -\sum_{j=m(t)+1}^{N}\log(1+\tau_j F^j_t). \tag{2.16}$$

Now, by Ito's formula, we can write the dynamics of $\log(1+\tau_j F^j_t)$ as:

$$d\log(1+\tau_j F^j_t) = \frac{\tau_j}{1+\tau_j F^j_t}dF^j_t.$$

Thus, equation (2.16) becomes:

$$\frac{dB(t,T_N)}{B(t,T_N)} = -\sum_{j=m(t)+1}^{N}\frac{\tau_j\sigma_j(t)F^j_t}{1+\tau_j F^j_t}dW^N_j(t).$$

Substituting this into (2.12) results in:

$$\frac{dZ^{T_N}(t)}{Z^{T_N}(t)} = \sqrt{\epsilon_t}dW^N_x(t) + \sum_{j=m(t)+1}^{N}\frac{\tau_j\sigma_j(t)F^j_t}{1+\tau_j F^j_t}dW^N_j(t). \tag{2.17}$$

Thus we now have dynamics for the forward price under the $T_N$-measure.

## 2.3 Approximation of the Hybrid Model

Now that we have the dynamics for the forward price under the $T_N$-measure, we are able to specify a characteristic function for the model. The reason we would want to do this is because Fourier inversion pricing techniques, which are highly efficient for model calibration, require a characteristic function to be used. This is

generally the case when no closed-form solution exists.

The process of finding a closed form characteristic function can be relatively cumbersome. Instead, one would look to using the methods proposed by Duffie *et al.* (2000). The problem here, however, is that this method requires the dynamics of the model to be affine. However, for the dynamics derived in (2.17), there are non-affine terms of the form $\frac{F_t^j}{1+\tau_j F_t^j}$. As a result, we need to introduce approximations for the model that simplify the dynamics to the point where we can specify a characteristic function. Once again, the bulk of the proof in this section comes from Grzelak and Oosterlee (2012).

First, we write:

$$\frac{dZ^{T_N}(t)}{Z^{T_N}(t)} = \sqrt{\epsilon_t} dW_x^N(t) + \sum_{j=m(t)+1}^{N} \psi_j(t) dW_j^N(t),$$

where

$$\psi_j(t) := \frac{s_j \sigma_j(t) F_t^j}{1 + s_j F_t^j}.$$

Now define $X_t := \log Z^{T_N}(t)$. By Ito's formula we can write:

$$\begin{aligned} dX_t &= \frac{1}{Z^{T_N}(t)} dZ^{T_N}(t) - \frac{1}{2}\Big(\frac{1}{Z^{T_N}(t)}\Big)^2 (dZ^{T_N}(t))^2, \\ &= \sqrt{\epsilon_t} dW_x^N(t) + \sum_{j=m(t)+1}^{N} \psi_j(t) dW_j^N(t), \\ &\quad - \frac{1}{2}\Big(\sqrt{\epsilon_t} dW_x^N(t) + \sum_{j=m(t)+1}^{N} \psi_j(t) dW_j^N(t)\Big)^2. \end{aligned}$$

Using the following formula:

$$\Big(\sum_{i=1}^{N} x_i\Big)^2 = \sum_{i=1}^{N} x_i^2 + \sum_{i=1}^{N} \sum_{j \neq i}^{N} x_i x_j,$$

and, by taking $x_j := \psi_j(t) dW_j^N(t)$, we can write

$$\begin{aligned} dX_t &= \sqrt{\epsilon_t} dW_x^N(t) + \sum_{j=m(t)+1}^{N} \psi_j(t) dW_j^N(t) \\ &\quad - \frac{1}{2}\Big(\epsilon_t + 2\sqrt{\epsilon_t} \sum_{j=m(t)+1}^{N} \psi_j(t) \rho_{x,j} + \sum_{j=m(t)+1}^{N} \psi_j^2(t) \\ &\quad + \sum_{i,j=m(t)+1, i \neq j}^{N} \psi_j(t) \psi_i(t) \rho_{i,j}\Big) dt. \end{aligned} \tag{2.18}$$

Now, define:

$$A_1(t) := \sum_{j=m(t)+1}^{N} \psi_j^2(t) + \sum_{i,j=m(t)+1, i\neq j}^{N} \psi_j(t)\psi_i(t)\rho_{i,j},$$
$$A_2(t) := \sum_{j=m(t)+1}^{N} \psi_j(t)\rho_{x,j}.$$

These definitions allow us to simplify (2.18) to:

$$dX_t = \sqrt{\epsilon_t} dW_x^N(t) + \sum_{j=m(t)+1}^{N} \psi_j(t) dW_j^N(t) - \frac{1}{2}\Big(\epsilon_t + 2\sqrt{\epsilon_t}A_2(t) + A_1(t)\Big)dt.$$

In order to use the result in Duffie *et al.* (2000), we require that $X_t$ is affine on the state vector, $\mathbf{Y}_t := [X_t, \epsilon_t, F_t^1, F_t^2, \ldots, F_t^N]^T$. Clearly $X_t$ is not affine on the state vector, as it includes terms of the form $\sqrt{\epsilon_t}$ in the drift. We therefore need to introduce some approximations to linearise these terms.

## 2.4 Hybrid Model Linearisation

We now look to linearise the non-affine terms in the dynamics of $X_t$. We use the same methods used in Grzelak and Oosterlee (2012) at this point. Alternative methods are explored in Section 4.2. The $\sqrt{\epsilon_t}$ term can be linearised by its first moment:

$$\sqrt{\epsilon_t} \approx \mathbb{E}[\sqrt{\epsilon_t}].$$

Using a combination of the results in Dufresne (2001) and Kummer (1936), we have a closed form solution for the expectation of a square-root process. However, this solution is very computationally expensive, which would directly affect the efficiency of the implementation of the final characteristic function. As a result, a proxy for the evaluation of the above function is relevant, namely:

$$\begin{aligned}\mathbb{E}[\sqrt{\epsilon_t}] &\approx a + be^{-ct}, \\ &=: \vartheta(t),\end{aligned} \tag{2.19}$$

where $a$, $b$, and $c$ are all constants. The derivation of these values can be found in Appendix A. Their final values can be found in (A.2), (A.3), and (A.4).

The other terms that require linearisation are the $A_1(t)$ and $A_2(t)$ terms, which both depend on $\psi_j(t)$. These $\psi_j(t)$ terms are a non-linear combination of $F_j(t)$. The linearisation of these terms can be done by freezing the LIBOR rates (Grzelak and

Oosterlee (2011), Hull and White (2000), Jäckel and Rebonato (2000)). This implies approximating the current LIBOR rate, $F_t^j$, by its initial rate i.e.

$$F_t^j \approx F_0^j,$$

which subsequently allows us to write the dynamics of $F_t^j$ as

$$dF_t^j \approx -\sigma_i(t)F_0^j \sum_{j=k+1}^{N} \psi_j(t)\rho_{k,j}dt + \sigma_i(t)F_0^j dW_j^N(t).$$

We are essentially approximating the LIBOR dynamics using arithmetic Brownian motions. This freezing of the LIBOR rates results in $\psi_j(t)$, $A_1(t)$ and $A_2(t)$ becoming affine in $F_t^j$.

Now that we have linearised the non-affine terms in the dynamics of $X_t$, we can identify a characteristic function. Per Duffie *et al.* (2000), the characteristic function for $X_t$, for a given state vector, $\mathbf{Y}_t = [X_t, \epsilon_t, F_t^1, F_t^1, \ldots, F_t^N]^T$, will be of the following form:

$$\phi^{T_N}(u, \mathbf{Y}_t, \tau) = \exp(A(u,\tau) + B(u,\tau)\mathbf{Y}_t),$$

where $A$ and $B$ satisfy the following system of ODEs:

$$\frac{\partial}{\partial \tau}B(u,\tau) = a_1^T B(u,\tau) + \frac{1}{2}B(u,\tau)^T c_1 B(u,\tau), \tag{2.20}$$

$$\frac{\partial}{\partial \tau}A(u,\tau) = B(u,\tau)^T a_0 + \frac{1}{2}B(u,\tau)^T c_0 B(u,\tau), \tag{2.21}$$

subject to the terminal condition $\phi^{T_N}(u, \mathbf{Y}_{T_N}, 0) = \exp(iuX_{T_N})$. The $a_i$ and $c_i$ terms are defined by:

$$\mu(\mathbf{Y}_t) = a_0 + a_1\mathbf{Y}_t, \tag{2.22}$$

$$(\Sigma(\mathbf{Y}_t)\Sigma(\mathbf{Y}_t)^T)_{ij} = (c_0)_{ij} + (c_1)_{ij}\mathbf{Y}_t. \tag{2.23}$$

For $(a_0, a_1) \in \mathbb{R}^n \times \mathbb{R}^{n\times n}$ and $(c_0, c_1) \in \mathbb{R}^{n\times n} \times \mathbb{R}^{n\times n\times n}$. The size of the state vector, $\mathbf{Y}_t$, is $n = N + 2$. Note that the left-hand terms in the above equations come directly from the dynamics of $\mathbf{Y}_t$:

$$\begin{aligned} d\mathbf{Y}_t &= \mu(\mathbf{Y}_t)dt + \Sigma(\mathbf{Y}_t)d\hat{W}^N(t), \\ &= \begin{bmatrix} -\frac{1}{2}\Big(\epsilon_t + 2\sqrt{\epsilon_t}A_2(t) + A_1(t)\Big) \\ \kappa(\bar{\epsilon} - \epsilon_t) \\ -F_t^1\sigma_1(t)\sum_{j=2}^N \psi_j(t)\rho_{1,j} \\ -F_t^2\sigma_2(t)\sum_{j=3}^N \psi_j(t)\rho_{2,j} \\ \vdots \\ -F_t^{N-1}\sigma_{N-1}(t)\sum_{j=N}^N \psi_j(t)\rho_{N-1,j} \\ 0 \end{bmatrix} dt + \Sigma(\mathbf{Y}_t)d\hat{W}^N(t), \end{aligned}$$

where $d\hat{W}^N(t)$ is an $(N+2)$-dimensional Brownian motion, $\mu(\mathbf{Y}_t)$ is the drift process, and $\Sigma(\mathbf{Y}_t)$ is the volatility process such that $\Sigma(\mathbf{Y}_t)\Sigma(\mathbf{Y}_t)^T$ is the instantaneous covariance matrix for $\mathbf{Y}_t$. Thus, we need to determine the instantaneous covariance matrix, $\Sigma(\mathbf{Y}_t)\Sigma(\mathbf{Y}_t)^T$, in order to proceed. For a given state vector, $\mathbf{Y}_t$, this covariance matrix will be of the following form:

$$\Sigma(\mathbf{Y}_t)\Sigma(\mathbf{Y}_t)^T = \begin{bmatrix} \Sigma_{x,x} & \Sigma_{x,\epsilon} & \Sigma_{x,F^1} & \Sigma_{x,F^2} & \dots & \Sigma_{x,F^N} \\ \Sigma_{\epsilon,x} & \Sigma_{\epsilon,\epsilon} & 0 & 0 & \dots & 0 \\ \Sigma_{F^1,x} & 0 & \Sigma_{F^1,F^1} & \Sigma_{F^1,F^2} & \dots & \Sigma_{F^1,F^N} \\ \Sigma_{F^2,x} & 0 & \Sigma_{F^2,F^1} & \Sigma_{F^2,F^2} & \dots & \Sigma_{F^2,F^N} \\ \vdots & \vdots & \vdots & \vdots & \ddots & \vdots \\ \Sigma_{F^N,x} & 0 & \Sigma_{F^N,F^1} & \Sigma_{F^N,F^2} & \dots & \Sigma_{F^N,F^N} \end{bmatrix} \tag{2.24}$$

We can solve for the individual elements in the matrix by looking at the co-efficients of the covariation terms: $[V,Y]_t = dV_t dY_t$, where $V_t$ and $Y_t$ are elements in the state vector, $\mathbf{Y}_t$. Determining these covariations, and including the correlations used in (2.8), we get the following:

$$\begin{aligned} \Sigma_{x,x} &= \Big(\sqrt{\epsilon_t}dW_x^N(t) + \sum_{j=m(t)+1}^{N} \psi_j(t)dW_j^N(t)\Big)^2, \\ &= \Big(\epsilon_t + 2\sqrt{\epsilon_t}A_2(t) + A_1(t)\Big), \end{aligned}$$

$$\begin{aligned} \Sigma_{x,\epsilon} &= \Sigma_{\epsilon,x}, \\ &= (\gamma\sqrt{\epsilon_t}dW_\epsilon^N(t))\Big(\sqrt{\epsilon_t}dW_x^N(t) + \sum_{j=m(t)+1}^{N} \psi_j(t)dW_j^N(t)\Big), \\ &= \gamma\epsilon_t\rho_{x,\epsilon}, \end{aligned}$$

$$\begin{aligned} \Sigma_{\epsilon,\epsilon} &= (\gamma\sqrt{\epsilon_t}dW_\epsilon^N(t))(\gamma\sqrt{\epsilon_t}dW_\epsilon^N(t)), \\ &= \gamma^2\epsilon_t, \end{aligned}$$

$$\begin{aligned} \Sigma_{x,F^i} &= \Sigma_{F^i,x}, \\ &= (\sigma_i(t)F_0^i dW_i^N(t))\Big(\sqrt{\epsilon_t}dW_x^N(t) + \sum_{j=m(t)+1}^{N} \psi_j(t)dW_j^N(t)\Big), \\ &= \Big(\rho_{x,i}\sigma_i(t)F_0^i\sqrt{\epsilon_t} + \sigma_i(t)F_0^i \sum_{j=m(t)+1}^{N} \psi_j\rho_{i,j}\Big), \end{aligned}$$

$$\begin{aligned}\Sigma_{F^i,F^j} &= (\sigma_i(t)F_0^i dW_i^N(t))(\sigma_j(t)F_0^j dW_j^N(t)),\\ &= \rho_{i,j}\sigma_i(t)\sigma_j(t)F_0^i F_0^j.\end{aligned}$$

The $0$ terms all come from the fact that we have assumed that the asset volatilility process is independent of the LIBOR rates. Clearly by linearising the dynamics of $X_t$ we have linearised the terms in the covariance matrix as well.

We can now solve the ODEs presented in (2.20) and (2.21). A simplification of these ODEs can be found in Appendix B. This marks the first major difference between this dissertation and the article by Grzelak and Oosterlee (2012); because they include a volatility term in the LIBOR framework, which is then part of the state vector, the drift term in the frozen LIBOR dynamics include terms which are relevant to the state vector. As a result, the $a_0$ term defined in Grzelak and Oosterlee (2012) has far more $0$'s than in this dissertation, while the $a_1$ term has far fewer $0$'s. As a result, the derivation of the final approximation model will begin to differ.

Observe that, as a result of the terminal condition, we require:

$$\begin{aligned}B_x(u,0) &= iu,\\ B_\epsilon(u,0) &= 0,\\ B_{F^j}(u,0) &= 0,\\ A(u,0) &= 0,\end{aligned}$$

and that, as a result of (B.1), we must have:

$$\begin{aligned}\frac{\partial}{\partial\tau}B_x(u,\tau) &= 0,\\ \frac{\partial}{\partial\tau}B_{F_j}(u,\tau) &= 0.\end{aligned}$$

These two results allow us to conclude that $B_{F^j}(u,\tau) = 0\ \forall\tau$, which further implies that the characteristic function does not include terms like $B_{F^j}(u,\tau)$ or $F_0^j$. This is of course a natural result of freezing the LIBOR rates (Grzelak and Oosterlee, 2012). These frozen rates behave like arithmetic Brownian motions, and no longer depend on their function value at a given time. As a result, the characteristic function used for this model will also not depend on these values.

Moreover, we can conclude that $B_x(u,\tau) = iu$. Using these two conclusions, we can re-write the system of ODEs as follows:

$$\phi^{T_N}(u, \mathbf{Y}_t, \tau) = \exp(A(u,\tau) + iuX_t + B_\epsilon(u,\tau)\epsilon_t), \tag{2.25}$$

where $A(u,\tau)$ and $B_\epsilon(u,\tau)$ satisfy the following system of ODEs:

$$\frac{\partial}{\partial\tau}B_\epsilon(u,\tau) = -\frac{1}{2}(u^2+iu) + (iu\rho_{x,\epsilon}\gamma - \kappa)B_\epsilon(u,\tau) + \frac{1}{2}\gamma^2 B_\epsilon^2(u,\tau), \tag{2.26}$$

$$\frac{\partial}{\partial\tau}A(u,\tau) = -(u^2+iu)\Big(\vartheta(t)A_2(t) + \frac{1}{2}A_1(t)\Big) + \kappa\bar{\epsilon}B_\epsilon(u,\tau), \tag{2.27}$$

subject to the terminal conditions $A(u,0) = B_\epsilon(u,0) = 0$.

## 2.5 Solving the System of ODEs

Due to the approximations that have been introduced, we have been able to significantly simplify the characteristic function of the log-forward process. We now look to determining solutions for these functions.

First observe that, due to Duffie *et al.* (2000), we can conclude that $B_\epsilon(u,\tau)$ and $A(u,\tau)$ are of Heston type (Heston, 1993). This means that analytic solutions exist for these functions, for constant parameters. However, it is important to note that both $A_1(t)$ and $A_2(t)$ are not constant, but piece-wise constant if we make the assumption that the interest rate volatility term, $\sigma_k(t)$, as well as the correlation terms $\rho_{x,k}$ and $\rho_{i,k}$ are constant. We shall proceed with the derivation assuming the $\sigma_k(t)$, $\rho_{x,k}$ and $\rho_{i,k}$ are indeed constant; however, changing this assumption to allow for a deterministic volatility and correlation structure would not be difficult. Only (2.29) would need to be re-evaluated. As a result of the piece-wise constant nature of $A_1(t)$ and $A_2(t)$, we need to take a different approach to solving the ODE's given in (2.26) and (2.27). As indicated by Wu and Zhang (2008), an analytic solution does indeed exist for piece-wise constant parameters as well. However, this solution is not constant, but recursive. We now derive this solution.

The trick that we will employ here is to solve the given ODE's for general initial conditions. The idea is to set up a recursive relationship between the function value at the beginning of the period, and the function value over the period for which it is constant.

We first re-write (2.26) and (2.27) as:

$$\frac{\partial}{\partial\tau}B_\epsilon(u,\tau) = b_0 + b_1 B_\epsilon(u,\tau) + b_2 B_\epsilon^2(u,\tau), \tag{2.28}$$

$$\frac{\partial}{\partial\tau}A(u,\tau) = A_0 + A_1 B_\epsilon(u,\tau), \tag{2.29}$$

where:

$$b_0 = -\frac{1}{2}(u^2+iu), \quad b_1 = (iu\rho_{x,\epsilon}\gamma - \kappa), \quad b_2 = \frac{1}{2}\gamma^2,$$
$$A_0 = -(u^2+iu)\Big(\vartheta(t)A_2(t) + \frac{1}{2}A_1(t)\Big), \quad A_1 = \kappa\bar{\epsilon}.$$

Observe that (2.29) depends on $A(u,\tau)$ and $B_\epsilon(u,\tau)$, while (2.28) only depends on $B_\epsilon(u,\tau)$. Thus, we solve (2.28) first.

Suppose that we are trying to solve the given ODEs over an interval, $[\tau_{j-1},\tau_j]$, where $A_1(t)$ and $A_2(t)$ are constant. Let $Y_1$ be the solution to:

$$0 = Y_1^2 b_2 + Y_1 b_1 + b_0.$$

Clearly we have

$$Y_1 = \frac{-b_1 \pm d}{2b_2},$$

where $d = \sqrt{b_1^2 - 4b_2b_0}$. Given that we only need one particular solution to the above we can, without loss of generality, let $Y_1 = \frac{-b_1-d}{2b_2}$.

Now define $Y_2 := B_\epsilon(u,\tau) - Y_1$. Because $Y_1$ is a constant in $\tau$, we must have

$$\frac{\partial}{\partial\tau}B_\epsilon(u,\tau) = \frac{\partial}{\partial\tau}Y_2.$$

Thus, we can write:

$$\begin{aligned}\frac{\partial}{\partial\tau}Y_2 &= (Y_1+Y_2)^2 b_2 + (Y_1+Y_2)b_1 + b_0,\\ &= b_2(Y_2^2 + 2Y_1Y_2 + Y_1^2) + (Y_1+Y_2)b_1 + b_0,\\ &= b_2(Y_2^2 + 2Y_2Y_1) + Y_2 b_1,\\ &= b_2 Y_2^2 - dY_2,\end{aligned} \tag{2.30}$$

with the initial condition $Y_2(0) = B(u,\tau_0) - Y_1$. Clearly $Y_2$ belongs to the family of Bernoulli differential equations (for constant parameters), and therefore has an explicit solution. Define $v := Y_2^{-1}$; this means that

$$\frac{\partial}{\partial \tau} v = -Y_2^{-2} \frac{\partial}{\partial \tau} Y_2,$$

which allows us to re-write (2.30) as:

$$\frac{\partial}{\partial \tau} v = -b_2 + dv.$$

Re-arranging, and using an integrating factor of $e^{-d\tau}$, allows us to write:

$$\begin{aligned} ve^{-d\tau} &= \frac{b_2}{d} e^{-d\tau} + C, \\ \implies v &= \frac{b_2}{d} + Ce^{d\tau}, \end{aligned} \tag{2.31}$$

where $C$ is the constant of integration. Using the initial condition, solving for $C$ yields:

$$\begin{aligned} C &= \frac{2b_2 d - b_2(2B_\epsilon(u,0)b_2 + b_1 + d)}{d(2B_\epsilon(u,0)b_2 + b_1 + d)}, \\ &= \frac{-b_2}{dg}, \end{aligned}$$

where $g = \frac{2B_\epsilon(u,0)b_2 + b_1 + d}{2B_\epsilon(u,0)b_2 + b_1 - d}$. Substituting this, as well as the expression for $v$, back into into (2.31) gives

$$Y_2 = \frac{-dge^{-d\tau}}{b_2(1 - ge^{-d\tau})}.$$

We can now determine $B_\epsilon(u,\tau)$ as follows:

$$\begin{aligned} B_\epsilon(u,\tau) &= Y_1 + Y_2 \\ &= \frac{-b_1 - d}{2b_2} + \frac{-dge^{-d\tau}}{b_2(1 - ge^{-d\tau})}, \\ &= \frac{(-b_1 - d - 2B_\epsilon(u,0)b_2 + 2B_\epsilon(u,0)b_2)(1 - ge^{\pm d\tau}) - 2dge^{-d\tau}}{2b_2(1 - ge^{-d\tau})}, \\ &= B_\epsilon(u,0) + \frac{(-b_1 - d - 2B_\epsilon(u,0)b_2)(1 - e^{-d\tau})}{2b_2(1 - ge^{-d\tau})}. \end{aligned}$$

Now that we have an expression for $B_\epsilon(u,\tau)$, we can determine $A(u,\tau)$. The evaluation of the integral of $A(u,\tau)$ can be found in Appendix C. If we now take $A(u,0)$ and $B_\epsilon(u,0)$ to be the value of the function at the beginning of the interval over which the parameter values are constant, we have a means of evaluating the ODEs over disjoint periods. Note that $\int_0^\tau \vartheta(s)ds$ is known in closed form.

We can now substitute the values for $A_0$, $A_1$, $b_0$, $b_1$ and $b_2$ back into the above expressions. Doing this results in the following characteristic function for the approximation of the forward price:

$$\phi^{T_N}(u, \mathbf{Y}_t, \tau) = \exp(A(u,\tau) + iuX_t + B_\epsilon(u,\tau)\epsilon_t),$$

where

$$B_\epsilon(u,\tau_j) = B_\epsilon(u,\tau_{j-1}) + \frac{(-(iu\rho_{x,\epsilon}\gamma - \kappa) - d - B_\epsilon(u,\tau_{j-1})\gamma^2)(1 - e^{-d(\tau_j - \tau_{j-1})})}{\gamma^2(1 - g_j e^{-d(\tau_j - \tau_{j-1})})},$$

$$A(u,\tau_j) = A(u,\tau_{j-1}) - (u^2 + iu)\Big(A_2(t)\int_{\tau_{j-1}}^{\tau_j} \vartheta(s)ds + \frac{1}{2}A_1(t)(\tau_j - \tau_{j-1})\Big)$$
$$+ \frac{\kappa\bar{\epsilon}}{\gamma^2}\Big((-(iu\rho_{x,\epsilon}\gamma - \kappa) - d)(\tau_j - \tau_{j-1}) - 2\log\Big[\frac{1 - g_j e^{-d(\tau_j - \tau_{j-1})}}{1 - g_j}\Big]\Big),$$

and

$$d = \sqrt{(iu\rho_{x,\epsilon}\gamma - \kappa)^2 + \gamma^2(u^2 + iu)},$$
$$g_j = \frac{B_\epsilon(u,\tau_{j-1})\gamma^2 + (iu\rho_{x,\epsilon}\gamma - \kappa) + d}{B_\epsilon(u,\tau_{j-1})\gamma^2 + (iu\rho_{x,\epsilon}\gamma - \kappa) - d}.$$

Because the above function steps through $\tau$ and not $t$, we need to be careful when evaluating the piece-wise constant functions. For example, suppose we are evaluating the characteristic function over the period $\tau_0$ to $\tau_1$. This corresponds to the period $T_{N-1}$ to $T_N$. Now, the piece-wise constant functions are fixed over the interval $[T_{N-1}, T_N)$, which corresponds to $(\tau_0, \tau_1]$. In other words, when implementing the model and stepping through $\tau$, the value of the piece-wise constant functions is determined by the value of $\tau$ at the end of the interval, not the beginning of the interval. Thus, $A_1(t)$ and $A_2(t)$ hold for $t = T_N - \tau_j$.

# Chapter 3

# Results from the Replication of the H1-LMM Model and the Implementation of the Newly Derived Model

In this section we present the results of the implementation of the model in Grzelak and Oosterlee (2012), as well as the implementation of the constant volatility variant using the same parameter values as those used in that paper. A comparison will then be made between these values and the market prices, which can be found in Appendix D.

## 3.1 Pricing Using the H-LMM

Before we present the results, we first need to present the pricing formula used to test the characteristic functions. The price of a vanilla call option, under the $T_N$-measure is as follows:

$$\begin{aligned} C(S_t, K) &= B(t, T_N)\mathbb{E}^{T_N}[(Z^{T_N} - K)^+ | \mathcal{F}_t], \\ &= S_t P_1 - K B(t, T_N) P_2, \end{aligned}$$

where $C(S_t, K)$ is the time $t$ price of the call option for a strike of $K$ and a current asset price of $S_t$ and

$$\begin{aligned} P_1 &= \mathbb{P}^{Z^{T_N}}(S_t > K), \\ P_2 &= \mathbb{P}^{T_N}(S_t > K). \end{aligned}$$

Define $\varphi(u,\tau)$ to be the characteristic function of $Z^{T_N}$ under its own measure. We must have

$$\varphi(u,\tau) = \frac{\phi(u-i,\tau)}{\phi(-1,\tau)}.$$

Then, using the Gil-Pelaez Theorem, we can re-write $P_1$ and $P_2$ as (Gil-Pelaez, 1951):

$$P_1 = \frac{1}{2} + \frac{1}{\pi}\int_0^\infty \mathrm{Re}\Big(\frac{e^{iu\log(K)}\phi(u-i,\tau)}{iu\phi(-i)}\Big)du,$$
$$P_2 = \frac{1}{2} + \frac{1}{\pi}\int_0^\infty \mathrm{Re}\Big(\frac{e^{iu\log(K)}\phi(u,\tau)}{iu}\Big)du,$$

where $\mathrm{R}(x)$ denotes the real part of $x$. The parameter values used by Grzelak and Oosterlee (2012) are:

$$\sigma_k = 0.25,\ \lambda = 1,\ \eta = 0.1, \tag{3.1}$$

while the initial forward curve is implied using the bond prices supplied by Grzelak and Oosterlee (2012), which can be found in Appendix D.

The parameter values for the equity part of the model are:

$$\kappa = 1.2,\ \bar{\epsilon} = 0.1,\ \gamma = 0.5,\ S_0 = 0.1,\ \epsilon_0 = 0.1. \tag{3.2}$$

The call prices for this section of the results comparison were calculated using the following maturities: $\mathcal{T} = \{T_2, T_5, T_{10}\}$, which corresponds to call options with 2, 5 and 10 year maturities. An effective upper bound of integration of $u = 30$ was used to evaluate the integrals in $P_1$ and $P_2$, with a grid containing 1000 points.

## 3.2 Replication of the H1-LMM Results

In this section we present the attempt to replicate the results presented in Grzelak and Oosterlee (2012) with regards to call prices.

The replication results in Table 3.1 give a mean absolute error of 4.13%, and gives a mean relative error of -1.28%. This is suggestive of a consistent over and under approximation of the market values. Note that both the mean absolute error and the mean relative error were calculated using values rounded to the fourth decimal place, in order to ensure consistency between these results and those presented by Grzelak and Oosterlee (2012).

**Tab. 3.1:** Table showing article results and replicated results for the H1-LMM model

| Strike | European Call Price | | | | | |
|---|---|---|---|---|---|---|
| | $T_2$ | | $T_5$ | | $T_{10}$ | |
| | Replication | Article | Replication | Article | Replication | Article |
| 40% | 0.6418 | 0.6418 | 0.7017 | 0.7017 | 0.7820 | 0.7821 |
| 80% | 0.3304 | 0.3299 | 0.4638 | 0.4638 | 0.6198 | 0.6203 |
| 100% | 0.2156 | 0.2149 | 0.3730 | 0.3730 | 0.5556 | 0.5562 |
| 120% | 0.1340 | 0.1332 | 0.2993 | 0.2993 | 0.5001 | 0.5008 |
| 160% | 0.0490 | 0.0483 | 0.1933 | 0.1933 | 0.4100 | 0.4109 |
| 200% | 0.0188 | 0.0184 | 0.1268 | 0.1268 | 0.3408 | 0.3419 |
| 240% | 0.0080 | 0.0078 | 0.0849 | 0.0850 | 0.2868 | 0.2878 |

The results reported by Grzelak and Oosterlee (2012) give a mean absolute error of 4.36%, and a mean relative error of -1.495%. The difference in error terms may come from the difference in accuracy between the Gil-Pelaez method, and the method proposed by Fang and Oosterlee (2008) in determining call prices (Gil-Pelaez, 1951). It may also simply come from an incorrect implementation of the approximate characteristic function. However, if the source of additional error does come from the different methods used to determine the prices, then this would suggest that the bounds of integration used by Grzelak and Oosterlee (2012) are not wholly appropriate.

## 3.3 Results from the Constant LMM Model

The results from applying the constant volatility LMM model for the given parameter values are presented in Table 3.2. These results were rounded to 4 decimal places so that they are consistent the results given by Grzelak and Oosterlee (2012), and give a mean absolute error of 4.135% as well as a mean relative error of -1.28%. These errors are very similar to that of the H1-LMM model. Both models are adequately able to capture the market, and are sufficient to be used for calibration.

## 3.4 Results Depicting the Explosion of the H1-LMM Characteristic Function

The final set of results that are presented in this section illustrate the instability of the H1-LMM characteristic function. For this, we will use the same parameters as

**Tab. 3.2:** Table showing results from the constant volatility model and market data

| Strike | European Call Price | | | | | |
|---|---|---|---|---|---|---|
| | $T_2$ | | $T_5$ | | $T_{10}$ | |
| | ChF | Market | ChF | Market | ChF | Market |
| 40% | 0.6418 | 0.6420 | 0.7017 | 0.7020 | 0.7820 | 0.7790 |
| 80% | 0.3304 | 0.3290 | 0.4638 | 0.4610 | 0.6198 | 0.6120 |
| 100% | 0.2156 | 0.2120 | 0.3730 | 0.3680 | 0.5556 | 0.5460 |
| 120% | 0.1340 | 0.1310 | 0.2993 | 0.2930 | 0.5001 | 0.4890 |
| 160% | 0.0490 | 0.0510 | 0.1933 | 0.1880 | 0.4100 | 0.3970 |
| 200% | 0.0188 | 0.0230 | 0.1268 | 0.1250 | 0.3409 | 0.3280 |
| 240% | 0.0080 | 0.0120 | 0.0849 | 0.0860 | 0.2868 | 0.2750 |

above, except we now set $\rho_{x,i} = -0.94$.

**Tab. 3.3:** Table showing the results of the constant volatility model, specifically using $\rho_{x,i} = -0.94$

| Strike | European Call Price | | | | | |
|---|---|---|---|---|---|---|
| | $T_1$ | $T_2$ | $T_3$ | $T_4$ | $T_5$ | $T_{10}$ |
| 40% | 0.6203 | 0.6415 | 0.6618 | 0.6809 | 0.6986 | $-5.512\times10^{15}$ |
| 80% | 0.2711 | 0.3265 | 0.3728 | 0.4128 | 0.4482 | $3.507\times10^{15}$ |
| 100% | 0.1434 | 0.2089 | 0.2629 | 0.3092 | 0.35 | $5.108\times10^{15}$ |
| 120% | 0.0653 | 0.1255 | 0.1794 | 0.2273 | 0.2701 | $-1.03\times10^{14}$ |
| 160% | 0.012 | 0.0424 | 0.0802 | 0.1196 | 0.1583 | $5.782\times10^{15}$ |
| 200% | 0.0026 | 0.0155 | 0.037 | 0.0639 | 0.0934 | $4.736\times10^{15}$ |
| 240% | 0.0007 | 0.0064 | 0.0184 | 0.0357 | 0.0569 | $7.683\times10^{15}$ |
| 260% | 0.0004 | 0.0043 | 0.0133 | 0.0272 | 0.045 | $-5.099\times10^{15}$ |
| 300% | 0.0001 | 0.0021 | 0.0074 | 0.0165 | 0.0291 | $8.214\times10^{15}$ |

The values in Table 3.3, which were generated using the constant volatility LMM with the updated parameter values, are clearly not representative of call prices, given that the values are so large and, in some cases, negative. Thus, there is a clear numerical instability problem with the characteristic function as is, and this should be remedied. This explosion result is also inherent in the characteristic function derived in Grzelak and Oosterlee (2012). Thus, methods will be explored that can be used to remedy the situation in both cases.

# Chapter 4

# Model Analysis

We now look to determine the cause of the numerical instability in the characteristic function for the model approximation, and develop solutions to these problems.

## 4.1 Numerical Analysis of the Constant Volatility Model

### 4.1.1 Exponent of the Characteristic Function

Many of the parameters in the characteristic function are not constant through time, so an analysis of these parameters may be difficult. Instead, the non-constant parameters are treated as functions of time. Then, we limit the analysis to the periods where the parameters are constant. Thereafter, the analysis is generalised to a tenor of times, while shifting the focus of these parameters from being constant to being functions. We also focus the analysis of the characteristic function on its real part alone. From Euler's formula, the exponential of a non-real number has a real part which is between -1 and 1, so the non-real part of the exponent of the characteristic function cannot be the cause of explosions.

Figure (4.1) shows the exponent of the characteristic function of the vanilla model versus one that is adjusted using the method in Section 4.2.1. Observe that the adjusted model, which does not explode, has an exponent that is negative and decreasing. Conversely, the vanilla model has an exponent that is positive and increasing. This gives some indication of characteristics that we would like the exponent term to have to ensure that it is well behaved.

First, recall that the characteristic function for the approximate model is:

$$\phi^{T_N}(u, \mathbf{Y}(t), \tau) = \exp(A(u, \tau) + iuX(t) + B_\epsilon(u, \tau)\epsilon_t),$$

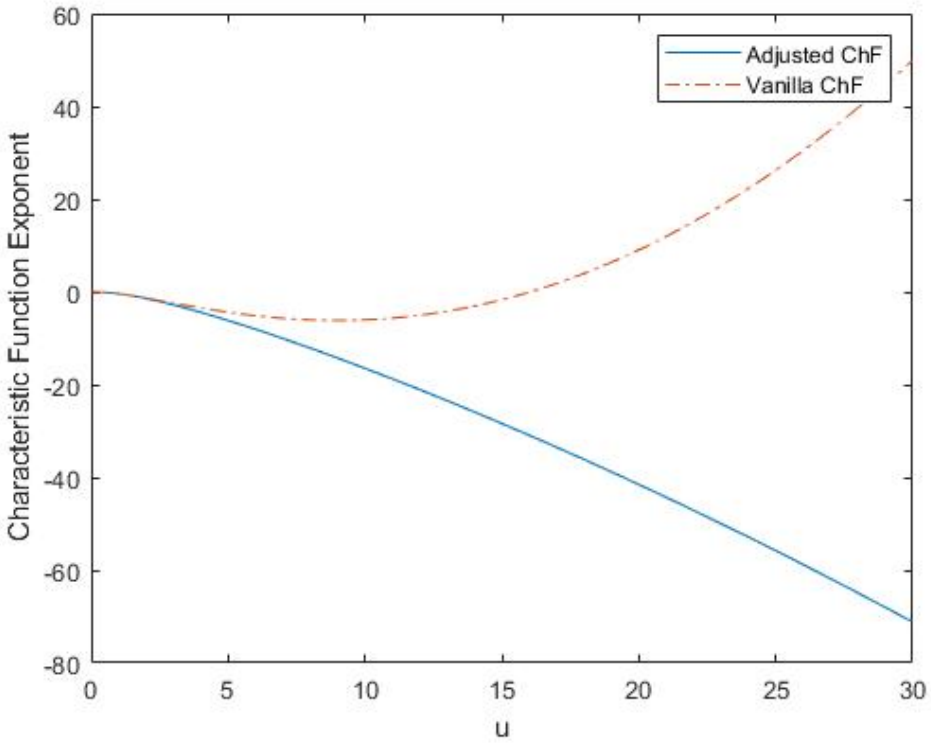


**Fig. 4.1:** Vanilla characteristic function exponent vs adjusted characteristic function exponent

where

$$B_\epsilon(u,\tau_j) = B_\epsilon(u,\tau_{j-1}) + \frac{(\kappa - iu\rho_{x,\epsilon}\gamma - d - B_\epsilon(u,\tau_{j-1})\gamma^2)(1-e^{-d(\tau_j-\tau_{j-1})})}{\gamma^2(1-g_j e^{-d(\tau_j-\tau_{j-1})})},$$

$$A(u,\tau_j) = A(u,\tau_{j-1}) - (u^2+iu)\Big(A_2(t)\int_{\tau_{j-1}}^{\tau_j}\vartheta(s)ds + \frac{1}{2}A_1(t)(\tau_j-\tau_{j-1})\Big)$$
$$+ \frac{\kappa\bar{\epsilon}}{\gamma^2}\Big((\kappa - iu\rho_{x,\epsilon}\gamma - d)(\tau_j-\tau_{j-1}) - 2\log\Big[\frac{1-g_j e^{-d(\tau_j-\tau_{j-1})}}{1-g_j}\Big]\Big),$$

and

$$d = \sqrt{(iu\rho_{x,\epsilon}\gamma-\kappa)^2 + \gamma^2(u^2+iu)},$$
$$g_j = \frac{B_\epsilon(u,\tau_{j-1})\gamma^2 + (iu\rho_{x,\epsilon}\gamma-\kappa) - d}{B_\epsilon(u,\tau_{j-1})\gamma^2 + (iu\rho_{x,\epsilon}\gamma-\kappa) + d}.$$

Now, the characteristic function is a function of $u$, the state vector and time. If we fix the starting point at time $0$, then the state vector input is fixed, and the characteristic function becomes a function of $u$ and $\tau$ only. Observe that the $d$ variable is a function of $u$, but is independent of $\tau$.

In the $B_\epsilon(u,\tau)$ equation, the sign of the next step is determined by $(\kappa - iu\rho_{x,\epsilon}\gamma - d - B_\epsilon(u,\tau_{j-1})\gamma^2)$. In this term, $d \geq \kappa$, which means that, at least the first $B_\epsilon(u,\tau_1) < 0$. Over time, because of the way that the addition to $B_\epsilon(u,\tau_{j-1})$ is scaled, the $B_\epsilon(u,\tau_j)$ term will always remain negative. This means that this term cannot be the cause of the explosion.

Moreover, because the $\frac{\kappa\bar{\epsilon}}{\gamma^2}\Big((\kappa - iu\rho_{x,\epsilon}\gamma - d)(\tau_j-\tau_{j-1}) - 2\log\Big[\frac{1-g_j e^{-d(\tau_j-\tau_{j-1})}}{1-g_j}\Big]\Big)$ term is the simplified integral of the $B_\epsilon(u,\tau)$ term, it will also be negative over time.

This leaves us with the first part of $A(u,\tau)$. Clearly the $u^2$ term is always positive. So, we need to look at the scenario where the remaining part of the term is negative.

First, define:

$$L(u,\tau) := -\Big(A_2(t)\int_{\tau_{j-1}}^{\tau_j}\vartheta(s)ds + \frac{1}{2}A_1(t)(\tau_j-\tau_{j-1})\Big).$$

Recall that the above holds when $t = T_N - \tau$, and that

$$A_1(t) = \sum_{j=m(t)+1}^{N}\psi_j^2(t) + \sum_{i,j=m(t)+1, i\neq j}^{N}\psi_j(t)\psi_i(t)\rho_{i,j},$$

$$A_2(t) = \sum_{j=m(t)+1}^{N}\psi_j(t)\rho_{x,j},$$

where

$$\psi_j(t) = \frac{s_j \sigma_j F_0^j}{1 + s_j F_0^j}.$$

Given our assumption that $F_0^j > 0$ and that we generally take $\sigma_i > 0$, we must have that $\psi_j(t) > 0$. Moreover, it is generally observed that forward rates have positive correlations i.e. $\rho_{i,j} > 0$ (Brigo and Mercurio, 2007). Thus, it is realistic to assume that $A_1(t) > 0$. A similar logic allows us to conclude that the sign of $A_2(t)$ is determined by the sign of $\rho_{x,i}$.

If the $L(u,\tau)$ function above is positive and increasing then the characteristic function will explode. Thus, we either require that it is positive and decreasing, or strictly negative.

We would like to determine the derivative of $L(u,\tau)$, in order to determine where this term is increasing or decreasing. First, for $\theta > \tau_{j-1}$, we have:

$$L(u,\theta) = -A_2(T_N - \tau_{j-1}) \int_{\tau_{j-1}}^{\theta} \vartheta(s) ds - \frac{1}{2} A_1(T_N - \tau_{j-1})(\theta - \tau_{j-1}),$$

$$\implies \frac{\partial}{\partial \theta} L(u,\theta) = -A_2(T_N - \tau_{j-1})\vartheta(\theta) - \frac{1}{2} A_1(T_N - \tau_{j-1}).$$

Now, take limits to the end of the period, just before the piece-wise constant parameters change:

$$\begin{aligned}\lim_{\theta \to \tau_j} \frac{\partial}{\partial \theta} L(u,\theta) &= \lim_{\theta \to \tau_j} \Big( - A_2(T_N - \tau_{j-1})\vartheta(\theta) - \frac{1}{2} A_1(T_N - \tau_{j-1}) \Big), \\ &= -A_2(T_N - \tau_{j-1})\vartheta(\tau_j) - \frac{1}{2} A_1(T_N - \tau_{j-1}).\end{aligned}$$

Thus, in order for $L(u,\tau)$ to be decreasing, we require:

$$\vartheta(\tau_j) \sum_{j=m(t)+1}^{N} \psi_j(t) \rho_{x,j} > -\frac{1}{2} A_1(T_N - \tau_{j-1}).$$

If we assume $\rho_{x,i} = \rho$ i.e. that the correlation is constant and equal, then we have:

$$\rho > \frac{-\frac{1}{2} A_1(T_N - \tau_{j-1})}{\vartheta(\tau_j) \sum_{j=(m(t)+1)}^{N} \psi_j(t)}.$$

Then, because the above expression assumed an arbitrary time point, and because we want this to hold for all $\tau$, we then set

$$\rho > \max_j \Big( \frac{-\frac{1}{2} A_1(T_N - \tau_{j-1})}{\vartheta(\tau_j) \sum_{j=(m(T_N - \tau_{j-1})+1)}^{N} \psi_j(T_N - \tau_{j-1})} \Big).$$

We can now look at the above in the case where $\tau$ becomes large. First, observe that:

$$\lim_{\tau \to \infty} \vartheta(\tau) = a.$$

Then, as $\sum_{j=(m(t)+1)}^{N} \psi_j(t) \geq \frac{1}{2} A_1(t)$, we can conclude that:

$$\rho > -\frac{1}{a}$$

This means that the range of values that $\rho$ is allowed to take on is informed by the value of $a$. Observe further that, if $a \to 0$, then the $L(u, \tau)$ is decreasing for all $\rho > -\infty$. In other words, we would require no restriction on the final value for $\rho$.

### 4.1.2 Instability Caused by the $\mathbb{E}[\sqrt{\epsilon_t}]$ Approximation

Interestingly, the approximation used for $\mathbb{E}[\sqrt{\epsilon_t}]$ adds an additional element of instability to the characteristic function. Observe from the definition of $c$, that if $b = 0$, then $c = -\infty$. In this case:

$$\vartheta(t) = \infty \; \forall t.$$

We can more generally state that

$$\lim_{b \to 0} \vartheta(t) = \infty.$$

Now, $b \to 0$ whenever:

$$\epsilon_0 \approx \bar{\epsilon} + \frac{\gamma^2}{8\kappa},$$

in which case, if we wanted to include this approximation, we would need to restrict the parameter values such that the above relationship can never hold.

## 4.2 Fixes for the Characteristic Function Instabilities

The aim of the above section was largely to illustrate the parameters that had the most influence on the instability. Clearly the $\rho_{x,i}$ parameter has a large affect on whether the characteristic function explodes or not. As a result, the whole $A_2(t) \int_{\tau_{j-1}}^{\tau_j} \vartheta(s) ds$ term will need to be managed.

Otherwise, the parameters that come from the dynamics of $\epsilon_t$ also have a major affect. However, all these parameters can be managed at once by using a different functional form for the $\mathbb{E}[\sqrt{\epsilon_t}]$ approximation term. Note that in Grzelak and Oosterlee (2012), the parameters in the dynamics for the volatility term in the LMM are also a problem for the same reason as in Section 4.1.2. The process of managing this is the same for $\epsilon_t$.

### 4.2.1 Re-arranging the Characteristic Function ODEs

We now re-arrange the differential equations so that the resulting solutions are generally more stable.

First, define $W(u,\tau)$ to be the solution to the differential equation defined by:

$$\frac{\partial}{\partial\tau}W(u,\tau) = \frac{\partial}{\partial\tau}A(u,\tau) + (iu+u^2)A_2(t)\vartheta(t),$$

and $P_\epsilon(u,\tau)$ to the solution to the differential equaiton defined by:

$$\frac{\partial}{\partial\tau}P_\epsilon(u,\tau) = \frac{\partial}{\partial\tau}B_\epsilon(u,\tau) - \frac{(iu+u^2)A_2(t)\vartheta(t)}{\epsilon_0}.$$

Next, observe that we can write the characteristic function for the differential equations in (2.25) as:

$$\begin{aligned}
\phi(u,\tau) &= \exp\Big(\int_0^\tau \frac{\partial}{\partial\tau}A(u,\tau)d\tau + iuX_0 + \epsilon_t\int_0^\tau \frac{\partial}{\partial\tau}B_\epsilon(u,\tau)d\tau\Big),\\
&= \exp\Big(iuX_t + \int_0^\tau \frac{\partial}{\partial\tau}A(u,\tau) + \epsilon_t\frac{\partial}{\partial\tau}B_\epsilon(u,\tau)d\tau\Big),\\
&= \exp\Big(iuX_0 + \int_0^\tau \frac{\partial}{\partial\tau}A(u,\tau) + \epsilon_t\frac{\partial}{\partial\tau}B_\epsilon(u,\tau) + (iu+u^2)A_2(t)\vartheta(t)\\
&\quad - (iu+u^2)A_2(t)\vartheta(t)d\tau\Big),\\
&= \exp\Big(iuX_0 + \int_0^\tau \frac{\partial}{\partial\tau}W(u,\tau) + \epsilon_t\frac{\partial}{\partial\tau}P_\epsilon(u,\tau)d\tau\Big).
\end{aligned}$$

The differential equation for $W(u,\tau)$ has been solved already: it is simply the differential equation for $A(u,\tau)$ with one less term. However, the differential equation for $P_\epsilon(u,\tau)$ is more difficult. With the inclusion of the $\vartheta(t)$ term, the co-efficients of $P_\epsilon(u,\tau)$ are no longer constant in which case there is no easy way to solve for $P_\epsilon(u,\tau)$. In fact, this differential equation is of the Ricatti form, which is notoriously difficult to solve without some particular solution.

Instead, we introduce another approximation that will aid in solving for the function $P_\epsilon(u,\tau)$. We approximate the asset variance process by the average of the integral over the period. In other words,

$$\begin{aligned}
\vartheta(t) &\approx \frac{1}{\tau_1-\tau_0}\int_{\tau_0}^{\tau_1}\vartheta(t)dt,\\
&= \frac{1}{\tau_1-\tau_0}\Big(a(\tau_1-\tau_0) - \frac{b}{c}(e^{-c\tau_1}-e^{-c\tau_0})\Big),\\
&=: \upsilon(\tau_1).
\end{aligned}$$

Note that this approximation will require either that a constant correlation structure is used for the asset-LIBOR correlation process, or that this correlation is also approximated as the average of its integral over the period.

With this approximation, we can re-write the solution to the characteristic function problem as:

$$\phi_A(u,\tau_j) = \exp\Big(W(u,\tau_j) + iuX_0 + \epsilon_0 Z_\epsilon(u,\tau)\Big),$$

$$\begin{aligned} W(u,\tau_j) &= W(u,\tau_{j-1}) - \frac{1}{2}(u^2+iu)A_1(t)(\tau_j-\tau_{j-1}) \\ &\quad + \frac{\kappa\bar{\epsilon}}{\gamma^2}\Big((-(iu\rho_{x,\epsilon}\gamma-\kappa)-d)(\tau_j-\tau_{j-1}) - 2\log\Big[\frac{1-g_j e^{-d(\tau_j-\tau_{j-1})}}{1-g_j}\Big]\Big), \\ Z_\epsilon(u,\tau_j) &= Z_\epsilon(u,\tau_{j-1}) + \frac{(-(iu\rho_{x,\epsilon}\gamma-\kappa)-d-B_\epsilon(u,\tau_{j-1})\gamma^2)(1-e^{-d(\tau_j-\tau_{j-1})})}{\gamma^2(1-g_j e^{-d(\tau_j-\tau_{j-1})})}, \end{aligned}$$

where

$$\begin{aligned} d &= \sqrt{(iu\rho_{x,\epsilon}\gamma-\kappa)^2 + \gamma^2(u^2+iu)\Big(2\frac{A_2(t)\upsilon(\tau_j)}{\epsilon_0}+1\Big)}, \\ g_j &= \frac{B_\epsilon(u,\tau_{j-1})\gamma^2 + (iu\rho_{x,\epsilon}\gamma-\kappa)+d}{B_\epsilon(u,\tau_{j-1})\gamma^2 + (iu\rho_{x,\epsilon}\gamma-\kappa)-d}. \end{aligned}$$

Incidentally, this stability adjustment can also be applied to the H1-LMM model presented by Grzelak and Oosterlee (2012) as well.

### 4.2.2 An SDE Based Approximation of $\mathbb{E}[\sqrt{\epsilon_t}]$

We now look at alternative functions that can be used to linearise $\mathbb{E}[\sqrt{\epsilon_t}]$.

As in Heston (1993), for an Ornstein-Uhlenbeck process of the form:

$$d\sqrt{\epsilon_t} = -\beta\sqrt{\epsilon_t}dt + \delta dW_t, \tag{4.1}$$

then, by Ito's formula, we have:

$$d\epsilon_t = (\delta^2 - 2\beta\epsilon_t)dt + 2\delta\sqrt{\epsilon_t}dW_t.$$

We can now set the above equal to the dynamics of $\epsilon_t$, in (2.2). Matching terms gives:

$$\beta_\epsilon = \frac{\kappa}{2}.$$

Then, from the expectation of the Ornstein-Uhlenbeck process in (4.1), we conclude:

$$\mathbb{E}[\sqrt{\epsilon_t}] \approx \sqrt{\epsilon_0} e^{-\frac{\kappa}{2}t}. \tag{4.2}$$

Due to the parameter restrictions required in (4.1), the above holds as an approximation. Specific restrictions would be needed for $\beta$ and $\delta$ for the expectation to hold in equality. In fact, we would require $\bar{\epsilon} = \frac{\gamma^2}{4\kappa}$ for the above to be exact. As a result, so long as the parameter values are non-zero, there will no longer be an opportunity for the approximation to result in a singularity.

As we will also implement the above for the H1-LMM we repeat the above process for the following dynamics:

$$dV(t) = \lambda(V(0) - V(t))dt + \eta\sqrt{V(t)}dW_t \qquad V_0 > 0.$$

This allows us to conclude:

$$\beta_V = \frac{\lambda}{2},$$

and

$$\mathbb{E}[\sqrt{V(t)}] \approx \sqrt{V(0)} e^{-\frac{\lambda}{2}t}.$$

### 4.2.3 An SDE Based Approximation With a More Sophisticated Parameter Estimation

Instead of directly using the SDE approach to inform the parameter values, we can also use this as an initial "guess" at a functional form for the estimate of $\mathbb{E}[\sqrt{\epsilon_t}]$, and combine this with the technique used by Grzelak and Oosterlee (2012) to estimate their parameter values. Doing this with the following approximation:

$$\mathbb{E}[\sqrt{\epsilon_t}] = a_\epsilon e^{-b_\epsilon t}. \tag{4.3}$$

we get:

$$\begin{aligned} a_\epsilon &= \sqrt{\epsilon_0}, \\ b_\epsilon &= -\log\left(\frac{\Lambda_\epsilon(1)}{a_\epsilon}\right), \end{aligned}$$

where $\Lambda_\epsilon(t)$ is defined in (A.1). This new approximation does not suffer the shortcomings of approximation (2.19), as it simply requires that $\sqrt{\epsilon_0} > 0$, which is assumed to be the case. This approximation is therefore consistent with the general model structure. Interestingly, the $a$ term above is the same as that of the SDE approach taken to determine parameter approximations. This suggests that the two

methods are reasonably consistent as well.

The fundamental difference between the functional forms of these approximations is that the original form converges to $a$ over time, while this new form converges to $0$. Converging to $0$ is desirable on account of the fact that $A_2(t)$ is increasing in $\tau$. This means that, if it isn't dampened by some other function, it will eventually result in $A(u, \tau)$ becoming greater than $0$ and consistently increasing thereafter.

Repeating this approximation for the stochastic volatility term in the LMM used by Grzelak and Oosterlee (2012), we have the following approximation:

$$\mathbb{E}[\sqrt{V(t)}] \approx a_v e^{-b_v t},$$

where

$$\begin{aligned} a_v &= \sqrt{V(0)}, \\ b_v &= -\log\left(\frac{\Lambda_v(t)}{a_v}\right). \end{aligned}$$

# Chapter 5

# Results from the Adjusted Models

In this section we present the results using the suggested model adjustments in Section 4. The results from these models will initially be compared, using the same parameter values as in Section 3, to the market values in Appendix D. Thereafter, they will be compared using the parameter values which are known to cause issues in the current model's characteristic function.

## 5.1 Comparison of the Adjusted Models with Market Prices

Here, we use the parameter values and tenor structure from (3.1) and (3.2) to compare the adjusted models in Sections 4.2.1, 4.2.2 and 4.2.3. These results are presented in Table 5.1.

The application of the adjustment in Section 4.2.1 results in a mean absolute error of 4.107% when compared to the market values with the same strike and maturity values as those provided by Grzelak and Oosterlee (2012). When applying the adjustment in Section 4.2.2, there is a mean absolute error of 4.02%. Interestingly, this is a lower error than is the case when using the old approximation for $\mathbb{E}[\sqrt{\epsilon_t}]$. This would imply that, even using this simple function, for the current model this new functional form of the approximation term is a better description than the old functional form. Finally, when applying the adjustment from Section 4.2.3, the mean absolute error is 3.58%, which is the lowest error achieved when implementing the constant volatility LMM. This is reasonable evidence that this new approximation function is more appropriate than the original. This is compounded by the fact that the implementation of this new approximation function is more efficient than that of the original.

**Tab. 5.1:** Table comparing results from the adjustments in Sections 4.2.1, 4.2.2 and 4.2.3

| **Strike** | **European Call Price** | | | | | | | | |
|---|---|---|---|---|---|---|---|---|---|
| | $T_2$ | | | $T_5$ | | | $T_{10}$ | | |
| | Section 4.2.1 | Section 4.2.2 | Section 4.2.3 | Section 4.2.1 | Section 4.2.2 | Section 4.2.3 | Section 4.2.1 | Section 4.2.2 | Section 4.2.3 |
| 40% | 0.6418 | 0.6418 | 0.6418 | 0.7018 | 0.7011 | 0.7015 | 0.7823 | 0.7784 | 0.7803 |
| 80% | 0.3298 | 0.3303 | 0.3300 | 0.4632 | 0.4613 | 0.4632 | 0.6194 | 0.6091 | 0.6150 |
| 100% | 0.2146 | 0.2156 | 0.2151 | 0.3718 | 0.3694 | 0.3721 | 0.5545 | 0.5414 | 0.5493 |
| 120% | 0.1326 | 0.1339 | 0.1333 | 0.2975 | 0.2949 | 0.2982 | 0.4984 | 0.4829 | 0.4925 |
| 160% | 0.0479 | 0.0489 | 0.0484 | 0.1908 | 0.1881 | 0.1921 | 0.4071 | 0.3882 | 0.4004 |
| 200% | 0.0183 | 0.0187 | 0.0185 | 0.1243 | 0.1217 | 0.1255 | 0.3371 | 0.3162 | 0.3300 |
| 240% | 0.0078 | 0.0080 | 0.0078 | 0.0828 | 0.0805 | 0.0839 | 0.2825 | 0.2606 | 0.2752 |

## 5.2 Comparison of the Adjusted Models with Updated Parameter Values

Now, we compare the results from the constant volatility model and the adjusted constant volatility model for the same parameter values, except for $\rho_{x,i} = -0.94$. This value of $\rho_{x,i}$ allows for the illustration of the numerical instability of the H1-LMM characteristic function, while ensuring that the instantaneous covariance matrix is still positive-definite. The instantaneous covariance matrix is not positive-definite for $\rho_{x,i}$ values close to $-1$. The result of using $\rho_{x,i} = -0.94$ is shown in Table 5.2. The shorter maturity prices are very similar, but there is a large deviation when applied to the longer dated options. This implies that, even though the ODE corrected method does reduce the instability, the additional approximation likely increases the error. The reason for this appears to stem from this method forcing the affect of the $A_2(t)$ term into the non-real part of the characteristic function when $\rho_{x,i}$ is negative. This is not observed with the adjusted approximation function method. However, because this function tends to $0$ over time, it reduces the affect of the $A_2(t)$ term to to zero over time. However, it does not diminish the affect of this term entirely, and from the outset. Thus, it would likely give a more accurate approximation of the H-LMM characteristic function.

There is also a large deviation when applying the adjustment method in Section 4.2.2 and Section 4.2.3. This suggests that approximation (4.2) does not diminish the affect of $A_2(t)$ as well as approximation (4.3).

**Tab. 5.2:** Table comparing results from the adjustments in Section 4.2.1, and using approximations (4.2) and (4.3), using $\rho_{x,i} = -0.94$

| **Strike** | **European Call Price** | | | | | |
|---|---|---|---|---|---|---|
| | $T_5$ | | | $T_{10}$ | | |
| | Adj (4.2.1) | Adj (4.2) | Adj (4.3) | Adj (4.2.1) | Adj (4.2) | Adj (4.3) |
| 40% | 0.6982 | 0.6994 | 0.6988 | 0.7694 | 0.7764 | 0.7731 |
| 80% | 0.4488 | 0.4528 | 0.4493 | 0.5815 | 0.6028 | 0.5914 |
| 100% | 0.3521 | 0.3571 | 0.3517 | 0.5049 | 0.5329 | 0.5172 |
| 120% | 0.2739 | 0.2793 | 0.2724 | 0.4386 | 0.4725 | 0.4528 |
| 160% | 0.164 | 0.1695 | 0.161 | 0.3326 | 0.3748 | 0.3489 |
| 200% | 0.0989 | 0.1039 | 0.096 | 0.2543 | 0.3009 | 0.2712 |
| 240% | 0.0609 | 0.0653 | 0.0589 | 0.1964 | 0.2444 | 0.213 |

# Chapter 6

# Application of the Characteristic Function Adjustments to the H1-LMM Model

In this section we review the affects of the characteristic function adjustment methods on the H1-LMM model. The same parameter values are used as in their article and in 3.2 and 3.1. The additional parameter values that were used by Grzelak and Oosterlee (2012) are as follows:

$$\lambda = 1, V(0) = 1, \eta = 0.1.$$

Note that the parameter values used for the additional approximations used in Grzelak and Oosterlee (2012) are found analogously to those used in Section 4.2.2 and 4.2.3.

**Tab. 6.1:** Table showing a sample of results from the H1-LMM model with the adjustment from Section 4.2.1 and market data

| **Strike** | **European Call Price** | | | | | |
|---|---|---|---|---|---|---|
| | $T_2$ | | $T_5$ | | $T_{10}$ | |
| | ChF | Market | ChF | Market | ChF | Market |
| 40% | 0.6418 | 0.642 | 0.7018 | 0.702 | 0.7823 | 0.779 |
| 80% | 0.3298 | 0.329 | 0.4632 | 0.461 | 0.6194 | 0.612 |
| 100% | 0.2146 | 0.212 | 0.3718 | 0.368 | 0.5545 | 0.546 |
| 120% | 0.1326 | 0.131 | 0.2975 | 0.293 | 0.4983 | 0.489 |
| 160% | 0.0479 | 0.051 | 0.1908 | 0.188 | 0.4071 | 0.397 |
| 200% | 0.0183 | 0.023 | 0.1243 | 0.125 | 0.3371 | 0.328 |
| 240% | 0.0078 | 0.012 | 0.0828 | 0.086 | 0.2825 | 0.275 |

The results from the application of the adjustment in Section 4.2.1 are presented

in Table 6.1. These results give a mean absolute error of 4.11%. This is still lower than the vanilla implementation which suggests that, for $\rho_{x,i} > 0$, this method is adequate.

**Tab. 6.2:** Table showing a sample of results from the H1-LMM model with the approximation adjustment (4.2) and market data

| **Strike** | **European Call Price** | | | | | |
|---|---|---|---|---|---|---|
| | $T_2$ | | $T_5$ | | $T_{10}$ | |
| | ChF | Market | ChF | Market | ChF | Market |
| 40% | 0.6418 | 0.642 | 0.7007 | 0.702 | 0.7778 | 0.779 |
| 80% | 0.3296 | 0.329 | 0.4591 | 0.461 | 0.6073 | 0.612 |
| 100% | 0.2143 | 0.212 | 0.3663 | 0.368 | 0.5391 | 0.546 |
| 120% | 0.1324 | 0.131 | 0.2910 | 0.293 | 0.4801 | 0.489 |
| 160% | 0.0477 | 0.051 | 0.1835 | 0.188 | 0.3846 | 0.397 |
| 200% | 0.0181 | 0.023 | 0.1172 | 0.125 | 0.3121 | 0.328 |
| 240% | 0.0076 | 0.012 | 0.0766 | 0.086 | 0.2563 | 0.275 |

The results from the application of the adjustment in Section 4.2.2 are presented in Table 6.2, which give a mean absolute error of 5.09%. This is the highest mean absolute error so far, which is evidence that the double approximation may be inappropriate. Thus, we apply the alternatively derived approximation function.

**Tab. 6.3:** Table showing a sample of results from the H1-LMM model with approximation adjustment (4.3) and market data

| **Strike** | **European Call Price** | | | | | |
|---|---|---|---|---|---|---|
| | $T_2$ | | $T_5$ | | $T_{10}$ | |
| | ChF | Market | ChF | Market | ChF | Market |
| 40% | 0.6418 | 0.642 | 0.7014 | 0.702 | 0.7800 | 0.779 |
| 80% | 0.3299 | 0.329 | 0.4625 | 0.461 | 0.6140 | 0.612 |
| 100% | 0.2148 | 0.212 | 0.3712 | 0.368 | 0.5479 | 0.546 |
| 120% | 0.1331 | 0.131 | 0.2971 | 0.293 | 0.4908 | 0.489 |
| 160% | 0.0482 | 0.051 | 0.1908 | 0.188 | 0.3983 | 0.397 |
| 200% | 0.0184 | 0.023 | 0.1243 | 0.125 | 0.3276 | 0.328 |
| 240% | 0.0078 | 0.012 | 0.0828 | 0.086 | 0.2727 | 0.275 |

Finally, the results from applying the adjustment in Section 4.2.3 are presented in Table 6.3. These results give a mean absolute error of 3.55%, which is the lowest across all the implementations relative to the sample of the market data. This

should be compared to the adjustment in Section 4.2.2, which resulted in the highest mean absolute error. Thus, it seems that the new functional form works for both of the volatility approximations. However, in the case of the H1-LMM model, one needs to be careful how one approximates the parameters in the final approximation function.

# Chapter 7

# Conclusion

The utility of the H-LMM model is without question; long-dated options cannot be sufficiently evaluated without some form of stochastic interest rate assumption nor can interest-equity products. However, the sheer number of parameters that need to be calibrated in this model results in the requirement of an efficient method of calibration. As such, the use of Fourier pricing techniques is paramount.

These Fourier techniques all require a characteristic function to be applied. Thus, having a characteristic function that is numerically unstable for a range of parameter values is a large drawback. This would require one to restrict the parameter values before use, severely limiting the potential of the final model.

Thus, the methods suggested in this dissertation are important in that they allow for efficient calibration techniques to be used, whilst not necessarily restricting the parameter values. Moreover, both cases of the adjusted approximation method are more efficient than the technique proposed by Grzelak and Oosterlee (2012), while approximation (4.3) has a lower error for the given data set.

While the ODE adjusted method ensures that the characteristic function does not explode, the additional approximation that is required to derive a closed-form solution results in the error term increasing relative to simply using the adjusted approximation method. Thus it is recommended to keep ODE method in mind should alternative characteristic functions need to be derived. However, there is sufficient evidence to conclude that the adjusted approximation method is more appropriate.

In sum, the adjusted approximation method is effective for the H1-LMM model characteristic function to be applied for calibration of the H-LMM model, as well as for the constant volatility LMM variant of the H-LMM model.

# Bibliography


Brigo, D. and Mercurio, F. (2007). *Interest rate models-theory and practice: With smile, inflation and credit*, Springer Science & Business Media.

Cox, J., Ingersoll, J. E. and Ross, S. A. (1985). A theory of the term structure of interest rates, *Econometrica* **53**: 385–407.

Duffie, D., Pan, J. and Singleton, K. (2000). Transform analysis and asset pricing for affine jump-diffusions, *Econometrica* **68**(6): 1343–1376.

Dufresne, D. (2001). *The integrated square-root process*, Working paper, University of Montreal.

Fang, F. and Oosterlee, C. W. (2008). A novel pricing method for European options based on Fourier-cosine series expansions, *SIAM Journal on Scientific Computing* **31**(2): 826–848.

Gil-Pelaez, J. (1951). Note on the inversion theorem, *Biometrika* **38**(3-4): 481–482.

Grzelak, L. A. and Oosterlee, C. W. (2011). On the Heston model with stochastic interest rates, *SIAM Journal on Financial Mathematics* **2**(1): 255–286.

Grzelak, L. A. and Oosterlee, C. W. (2012). An equity-interest rate hybrid model with stochastic volatility and the interest rate smile, *The Journal of Computational Finance* **15**(4): 1–33.

Heston, S. L. (1993). A closed-form solution for options with stochastic volatility with applications to bond and currency options, *The review of financial studies* **6**(2): 327–343.

Hull, J. C. and White, A. (2000). Forward rate volatilities, swap rate volatilities, and the implementation of the LIBOR market model.

Hull, J. and White, A. (1996). Using Hull-White interest rate trees, *Journal of derivatives* **3**(3): 26–36.

Jäckel, P. and Rebonato, R. (2000). Linking caplet and swaption volatilities in a BGM/J framework: Approximate solutions, *Quantitiative Research Centre, The Royal Bank of Scotland* .

Kummer, E. E. (1936). Über die hypergeometrische Reihe, *Journal für die reine und angewandte Mathematik* **15**: 39–83.

Piterbarg, V. V. (2005). Stochastic volatility model with time-dependent skew, *Applied Mathematical Finance* **12**(2): 147–185.

Wu, L. and Zhang, F. (2008). Fast swaption pricing under the market model with a square-root volatility process, *Quantitative Finance* **8**(2): 163–180.

# Appendix A

# Derivation of the Parameter Values in Equation (2.19)

We derive the parameter values for the expectation of the asset volatility process, as well as the parameters for the analogous approximation of the expectation of the interest rate volatility process used in Grzelak and Oosterlee (2012).

The dynamics for the relevant processes are:

$$\begin{aligned} d\epsilon_t &= \kappa(\bar{\epsilon} - \epsilon_t)dt + \gamma\sqrt{\epsilon_t}dW_\epsilon(t), \\ dV(t) &= \lambda(V(0) - V(t))dt + \eta\sqrt{V(t)}dW_V^N(t). \end{aligned}$$

Note that $\epsilon_t$ is the variance process of the underlying asset, while $V(t)$ is the variance process of the LMM. Note further that, with no stochastic volatility in the LMM, this simplifies considerably.

We use the following approximations:

$$\begin{aligned} \sqrt{\epsilon_t} &\approx \mathbb{E}[\sqrt{\epsilon_t}] = a_1 + b_1 e^{-c_1 t}, \\ \sqrt{V(t)} &\approx \mathbb{E}[\sqrt{V(t)}] = a_2 + b_2 e^{-c_2 t}. \end{aligned}$$

Define $\tilde{\Lambda}(t) := a + be^{-ct}$. We seek to optimise: $\min_{a,b,c} ||\Lambda(t) - \tilde{\Lambda}(t)||_n$, where $||\cdot||_n$ is any $n^{th}$ norm, and:

$$\Lambda(t) = \sqrt{c(t)(\omega(t) - 1) + c(t)d + \frac{c(t)d}{2(d + \omega(t))}}. \tag{A.1}$$

Now, for the case of $\epsilon_t$, we also have:

$$\begin{aligned} c_\epsilon(t) &= \frac{\gamma^2(1 - e^{-\kappa t})}{4\kappa}, \\ w_\epsilon(t) &= \frac{4\kappa\epsilon_0 e^{-\kappa t}}{\gamma^2(1 - e^{-\kappa t})}, \\ d_\epsilon &= \frac{4\kappa\bar{\epsilon}}{\gamma^2}. \end{aligned}$$

and for $V(t)$, we have:

$$\begin{aligned} c_V(t) &= \frac{\eta^2(1-e^{-\lambda t})}{4\lambda}, \\ w_V(t) &= \frac{4\lambda V(0)e^{-\lambda t}}{\eta^2(1-e^{-\lambda t})}, \\ d_V &= \frac{4\lambda V(0)}{\eta^2}. \end{aligned}$$

We now take limits as $t$ goes to $0$, $1$, and $+\infty$. This gives:

$$\begin{aligned} \lim_{t\to+\infty}\Lambda(t) &= \sqrt{\bar{\xi}-\frac{\gamma^2}{8\kappa}} = a_1 = \lim_{t\to+\infty}\tilde{\Lambda}(t), \\ \lim_{t\to 0}\Lambda(t) &= \sqrt{\xi(0)} = a_1+b_1 = \lim_{t\to 0}\tilde{\Lambda}(t), \\ \lim_{t\to 1}\Lambda(t) &= \Lambda(1) = a_1+b_1e^{-c_1t} = \lim_{t\to 1}\tilde{\Lambda}(t), \end{aligned}$$

and:

$$\begin{aligned} \lim_{t\to+\infty}\Lambda(t) &= \sqrt{V(0)-\frac{\eta^2}{8\lambda}} = a_1 = \lim_{t\to+\infty}\tilde{\Lambda}(t), \\ \lim_{t\to 0}\Lambda(t) &= \sqrt{V(0)} = a_2+b_2 = \lim_{t\to 0}\tilde{\Lambda}(t), \\ \lim_{t\to 1}\Lambda(t) &= \Lambda(1) = a_2+b_2e^{-c_2t} = \lim_{t\to 1}\tilde{\Lambda}(t). \end{aligned}$$

Re-arranging the above yields:

$$a_1 = \sqrt{\bar{\epsilon}-\frac{\gamma^2}{8\kappa}}, \tag{A.2}$$

$$b_1 = \sqrt{\epsilon_0}-a_1, \tag{A.3}$$

$$c_1 = -\log(\frac{\Lambda(1)-a_1}{b_1}), \tag{A.4}$$

and

$$\begin{aligned} a_2 &= \sqrt{V(0)-\frac{\eta^2}{8\lambda}}, \\ b_2 &= \sqrt{V(0)}-a_2, \\ c_2 &= -\log(\frac{\Lambda(1)-a_2}{b_2}). \end{aligned}$$

# Appendix B

# Simplification of (2.20) and (2.21)

Equation (2.22) can be re-written as:

$$\begin{bmatrix} -\frac{1}{2}\Big(\epsilon_t + 2\vartheta(t)A_2(t) + A_1(t)\Big) \\ \kappa(\bar{\epsilon} - \epsilon_t) \\ -F_0^1\sigma_1(t)\sum_{j=2}^{N}\psi_j(t)\rho_{1,j} \\ -F_0^2\sigma_2(t)\sum_{j=3}^{N}\psi_j(t)\rho_{2,j} \\ \vdots \\ -F_0^{N-1}\sigma_{N-1}(t)\sum_{j=N-1}^{N}\psi_j(t)\rho_{N-1,j} \\ 0 \end{bmatrix} = a_0 + a_1\mathbf{Y}(t),$$

$$= a_0 + a_1\begin{bmatrix} X(t) \\ \epsilon_t \\ L_1(t) \\ \vdots \\ L_N(t) \end{bmatrix}.$$

Thus we must have:

$$a_0 = \begin{bmatrix} -\frac{1}{2}\Big(2\vartheta(t)A_2(t) + A_1(t)\Big) \\ \kappa\bar{\epsilon} \\ -F_0^1\sigma_1(t)\sum_{j=2}^{N}\psi_j(t)\rho_{1,j} \\ -F_0^2\sigma_2(t)\sum_{j=3}^{N}\psi_j(t)\rho_{2,j} \\ \vdots \\ -F_0^{N-1}\sigma_{N-1}(t)\sum_{j=N}^{N}\psi_j(t)\rho_{N-1,j} \\ 0 \end{bmatrix},$$

and

$$a_1 = \begin{bmatrix} 0 & -\frac{1}{2} & 0 & \dots & 0 \\ 0 & -\kappa & 0 & \dots & 0 \\ 0 & 0 & 0 & \dots & 0 \\ \vdots & \vdots & \vdots & \ddots & \vdots \\ 0 & 0 & 0 & \dots & 0 \end{bmatrix}.$$

Next we re-write (2.23) as:

$$\Sigma_{i,j} = (c_0)_{ij} + (c_1)_{ij} \begin{bmatrix} X(t) \\ \epsilon_t \\ F_t^1 \\ \vdots \\ F_t^N \end{bmatrix},$$

where $\Sigma_{i,j} = (\Sigma(\mathbf{Y}(t))\Sigma(\mathbf{Y}(t))^T)_{ij}$. Now, $(c_0)_{i,j}$ is a scalar value, and $(c_1)_{i,j}$ is a $n \times 1$ vector. Let $c_1(i,j,k) = (((c_1)_{i,j})_k)$ be the $k^{\text{th}}$ element of the $(c_1)_{i,j}$ vector. The $k$ value corresponds to the variable being dealt with. As a result, $k = 1$ corresponds to $X_t$, $k = 2$ corresponds to $\epsilon_t$, and $k = j$ corresponds to $L_{j-2}(t)$ for $j > 2$.

This allows us to write (2.23) more generally as:

$$\Sigma_{i,j} = (c_0)_{ij} + \sum_{k=1}^{n} c_1(i,j,k)\mathbf{Y}_k(t).$$

Matching terms gives:

$$\begin{aligned} &c_1(1,1,2) = 1, \\ &c_1(1,2,2) = c_1(2,1,2) = \rho_{x,\epsilon}\gamma, \\ &c_1(2,2,2) = \gamma^2. \end{aligned}$$

This can be written in matrix form as:

$$c_1 = \begin{bmatrix} \begin{bmatrix} 0 \\ 1 \\ 0 \\ \vdots \\ 0 \end{bmatrix} & \begin{bmatrix} 0 \\ \rho_{x,\epsilon}\gamma \\ 0 \\ \vdots \\ 0 \end{bmatrix} & \mathbf{0} & \dots & \mathbf{0} \\ \begin{bmatrix} 0 \\ \rho_{x,\epsilon}\gamma \\ 0 \\ \vdots \\ 0 \end{bmatrix} & \begin{bmatrix} 0 \\ \gamma^2 \\ 0 \\ \vdots \\ 0 \end{bmatrix} & \mathbf{0} & \dots & \mathbf{0} \\ \mathbf{0} & \mathbf{0} & \mathbf{0} & \dots & \mathbf{0} \\ \vdots & \vdots & \vdots & \ddots & \vdots \\ \mathbf{0} & \mathbf{0} & \mathbf{0} & \dots & \mathbf{0} \end{bmatrix},$$

where $\mathbf{0}$ is a $(n \times 1)$-dimensional matrix of $0$'s.

We also have:

$$c_0 = \begin{bmatrix} 2\vartheta(t)A_2(t) + A_1(t) & 0 & \Sigma_{x,F^1} & \Sigma_{x,F^2} & \dots & \Sigma_{x,F^N} \\ 0 & 0 & 0 & 0 & \dots & 0 \\ \Sigma_{F^1,x} & 0 & \Sigma_{F^1,F^1} & \Sigma_{F^1,F^2} & \dots & \Sigma_{F^1,F^N} \\ \Sigma_{F_2,x} & 0 & \Sigma_{F^2,F^1} & \Sigma_{F^2,F^2} & \dots & \Sigma_{F_2,F^N} \\ \vdots & \vdots & \vdots & \vdots & \ddots & \vdots \\ \Sigma_{F^N,x} & 0 & \Sigma_{F^N,F^1} & \Sigma_{F^N,F^2} & \dots & \Sigma_{F^N,F^N} \end{bmatrix}.$$

First, observe that $B(u,\tau)$ can be written in terms of the components specific to each element in the state vector:

$$B(u,\tau) = \begin{bmatrix} B_x(u,\tau) \\ B_\epsilon(u,\tau) \\ B_{F^1}(u,\tau) \\ B_{F^2}(u,\tau) \\ \vdots \\ B_{F^N}(u,\tau) \end{bmatrix}.$$

Now, observe that:

$$a_1^T B(u,\tau) = -\frac{1}{2}B_x(u,\tau) - \kappa B_\epsilon(u,\tau),$$

and

$$
\begin{aligned}
&B(u,\tau)^T c_1 B(u,\tau) \\
&= \begin{bmatrix} \begin{bmatrix} 0 \\ B_x(u,\tau) + B_\epsilon(u,\tau)\rho_{x,\epsilon}\gamma \\ 0 \\ \vdots \\ 0 \end{bmatrix} \end{bmatrix}^T \\
&\quad = \begin{bmatrix} \begin{bmatrix} 0 \\ B_x(u,\tau)\rho_{x,\epsilon}\gamma + B_\epsilon(u,\tau)\gamma^2 \\ 0 \\ \vdots \\ 0 \end{bmatrix} \\ \mathbf{0} \\ \vdots \\ \mathbf{0} \end{bmatrix} B(u,\tau), \\
&= B_x(u,\tau) \begin{bmatrix} 0 \\ B_x(u,\tau) + B_\epsilon(u,\tau)\rho_{x,\epsilon}\gamma \\ 0 \\ \vdots \\ 0 \end{bmatrix} + B_\epsilon(u,\tau) \begin{bmatrix} 0 \\ B_x(u,\tau)\rho_{x,\epsilon}\gamma + B_\epsilon(u,\tau)\gamma^2 \\ 0 \\ \vdots \\ 0 \end{bmatrix}, \\
&= \begin{bmatrix} 0 \\ B_x(u,\tau)(B_x(u,\tau) + B_\epsilon(u,\tau)\rho_{x,\epsilon}\gamma) + B_\epsilon(u,\tau)(B_x(u,\tau)\rho_{x,\epsilon}\gamma + B_\epsilon(u,\tau)\gamma^2) \\ 0 \\ \vdots \\ 0 \end{bmatrix}.
\end{aligned}
$$

Then, we can write (2.20) as:

$$
\begin{aligned}
&\frac{\partial}{\partial\tau}B(u,\tau) = \\
&\begin{bmatrix} 0 \\ \frac{1}{2}B_x(u,\tau)(B_x(u,\tau)-1) + (B_x(u,\tau)\rho_{x,\epsilon}\gamma - \kappa)B_\epsilon(u,\tau) + \frac{1}{2}\gamma^2 B_\epsilon^2(u,\tau) \\ 0 \\ \vdots \\ 0 \end{bmatrix}. \qquad \text{(B.1)}
\end{aligned}
$$

Further observe that:

$$
\begin{aligned}
B(u,\tau)^T a_0 = &-\frac{1}{2}\Big(2\vartheta(t)A_2(t) + A_1(t)\Big)B_x(u,\tau) + \kappa\bar{\epsilon}B_\epsilon(u,\tau) \\
&- \sum_{i=1}^{N} \sigma_i(t) F_0^1 B_{F^i}(u,\tau) \sum_{j=i+1}^{N} \psi_j(t)\rho_{i,j},
\end{aligned}
$$

where $\sum_{i=N+1}^{N} := 0$. The final matrix multiplication required is:

$$
\begin{aligned}
&B(u,\tau)^T c_0 B(u,\tau) = \\
&\begin{bmatrix} (2\vartheta(t)A_2(t)+A_1(t))B_x(u,\tau) + \sum_{i=1}^{N} B_{F^i}(u,\tau)\Sigma_{F^i,x} \\ 0 \\ B_x(u,\tau)\Sigma_{x,F^1} + \sum_{i=1}^{N} B_{F_i}(u,\tau)\Sigma_{F^i,F^1} \\ \vdots \\ B_x(u,\tau)\Sigma_{x,F_N} + \sum_{i=1}^{N} \Sigma_{F^i,F^N} \end{bmatrix}^T B(u,\tau), \\
&= B_x(u,\tau)\Big((2\vartheta(t)A_2(t)+A_1(t))B_x(u,\tau) + \sum_{i=1}^{N} B_{F^i}(u,\tau)\Sigma_{F^i,x}\Big) \\
&+ \sum_{i=1}^{N} B_{F^i}(u,\tau)\Big(B_x(u,\tau)\Sigma_{x,F^i} + \sum_{j=1}^{N} B_{F^j}(u,\tau)\Sigma_{F^j,F^i}\Big), \\
&= (2\vartheta(t)A_2(t)+A_1(t))B_x^2(u,\tau) \\
&+ B_x(u,\tau)\sum_{i=1}^{N} B_{F^i}(u,\tau)\Big(\rho_{x,i}\sigma_i(t)F_0^i\vartheta(t) + \sigma_i(t)F_0^i \sum_{j=m(t)+1}^{N} \psi_j\rho_{i,j}\Big) \\
&+ \sum_{i=1}^{N} B_{F^i}(u,\tau)B_x(u,\tau)\Big(\rho_{x,i}\sigma_i(t)F_0^i\vartheta(t) + \sigma_i(t)F_0^i \sum_{j=m(t)+1}^{N} \psi_j\rho_{i,j}\Big) \\
&+ \sum_{i=1}^{N} B_{F^i}(u,\tau)\sum_{j=1}^{N} B_{F^j}(u,\tau)\rho_{i,j}\sigma_i(t)\sigma_j(t)F_0^iF_0^j
\end{aligned}
$$

Thus, we are able to write (2.21) as:

$$
\begin{aligned}
\frac{\partial}{\partial\tau}A(u,\tau) = B_x(u,\tau)(B_x(u,\tau)-1)\Big(\vartheta(t)A_2(t)+\frac{1}{2}A_1(t)\Big) + \kappa\bar{\epsilon}B_\epsilon(u,\tau) \\
+ \sum_{j=m(t)+1}^{N} B_x(u,\tau)B_{F^j}(u,\tau)\rho_{x,j}\sigma_j(t)F_0^j\vartheta(t) \\
+ \frac{1}{2}\sum_{j=m(t)+1}^{N} B_{F^j}^2(u,\tau)\sigma_j^2(t)(F_0^j)^2 \\
+ \sum_{i,j=m(t)+1,i\neq j}^{N} B_{F^j}(u,\tau)B_{F^j}(u,\tau)\sigma_j(t)\sigma_j(t)F_0^iF_0^j\rho_{i,j}.
\end{aligned}
$$

## Appendix C

# Integral of Equation (2.29)

Integrating (2.29) with respect to $\tau$ gives:

$$
\begin{aligned}
A(u,\tau) &= A(u,0) + \int_0^\tau A_0 ds + B_\epsilon(u,0)\tau + A_1 \int_0^\tau B_\epsilon(u,s) ds, \\
&= A(u,0) + \int_0^\tau -(u^2+iu)\Big(\vartheta(s)A_2(t) + \frac{1}{2}A_1(t)\Big) ds \\
&+ A_1 B_\epsilon(u,0)\tau + A_1 \frac{(-b_1 - d - 2B_\epsilon(u,0)b_2)}{2b_2} \int_0^\tau \frac{(1-e^{-ds})}{(1-ge^{-ds})} ds, \\
&= A(u,0) - (u^2+iu)\int_0^\tau \Big(\vartheta(s)A_2(t) + \frac{1}{2}A_1(t)\Big) ds + A_1 B_\epsilon(u,0)\tau \\
&+ A_1 \frac{(-b_1 - d - 2B_\epsilon(u,0)b_2)}{2b_2} \int_0^\tau \frac{(1-e^{-ds}) + ge^{-ds} - ge^{-ds}}{(1-ge^{-ds})} ds, \\
&= A(u,0) - (u^2+iu)\Big(A_2(t)\int_0^\tau \vartheta(s) ds + \frac{1}{2}A_1(t)\tau\Big) + A_1 B_\epsilon(u,0)\tau \\
&+ A_1 \frac{(-b_1 - d - 2B_\epsilon(u,0)b_2)}{2b_2} \Big(\tau - \int_0^\tau \frac{(1-g)e^{-ds}}{(1-ge^{-ds})} ds\Big), \\
&= A(u,0) - (u^2+iu)\Big(A_2(t)\int_0^\tau \vartheta(s) ds + \frac{1}{2}A_1(t)\tau\Big) + A_1 B_\epsilon(u,0)\tau \\
&+ A_1 \frac{(-b_1 - d - 2B_\epsilon(u,0)b_2)}{2b_2} \Big(\tau + \frac{(1-g)}{dg} \int_1^{e^{-d\tau}} \frac{g}{1-gu} du\Big), \\
&= A(u,0) - (u^2+iu)\Big(A_2(t)\int_0^\tau \vartheta(s) ds + \frac{1}{2}A_1(t)\tau\Big) + A_1 B_\epsilon(u,0)\tau \\
&+ A_1 \frac{(-b_1 - d + 2B_\epsilon(u,0)b_2)}{2b_2} \Big(\tau - \frac{(1-g)}{dg} \log\Big[\frac{1-ge^{-d\tau}}{1-g}\Big]\Big), \\
&= A(u,0) - (u^2+iu)\Big(A_2(t)\int_0^\tau \vartheta(s) ds + \frac{1}{2}A_1(t)\tau\Big), \\
&+ \frac{A_1}{2b_2}\Big((-b_1 - d)\tau - \frac{(-b_1 - d - 2B_\epsilon(u,0)b_2)(1-g)}{dg} \log\Big[\frac{1-ge^{-d\tau}}{1-g}\Big]\Big) \\
&= A(u,0) - (u^2+iu)\Big(A_2(t)\int_0^\tau \vartheta(s) ds + \frac{1}{2}A_1(t)\tau\Big) \\
&+ \frac{A_1}{2b_2}\Big((-b_1 - d)\tau - 2\log\Big[\frac{1-ge^{-d\tau}}{1-g}\Big]\Big),
\end{aligned}
$$

where the proof follows by noting that $A_1(t)$ and $A_2(t)$ are constant over the given interval.

# Appendix D

# Market data

## D.1 Zero Coupon Bond prices

**Tab. D.1:** ZCB prices

| **Bond** | **Price** |
|---|---|
| 0.9512 | $B(0,1)$ |
| 0.9048 | $B(0,2)$ |
| 0.8607 | $B(0,3)$ |
| 0.8187 | $B(0,4)$ |
| 0.7788 | $B(0,5)$ |
| 0.7408 | $B(0,6)$ |
| 0.7047 | $B(0,7)$ |
| 0.6703 | $B(0,8)$ |
| 0.6376 | $B(0,9)$ |
| 0.6065 | $B(0,10)$ |

## D.2 European Call Option Market Prices

**Tab. D.2:** European call market prices

| | **European Call Price** | | | | | |
|---|---|---|---|---|---|---|
| **Strike** | $T_1$ | $T_2$ | $T_3$ | $T_4$ | $T_5$ | $T_{10}$ |
| 40% | 0.62 | 0.642 | 0.663 | 0.683 | 0.702 | 0.779 |
| 80% | 0.271 | 0.329 | 0.378 | 0.421 | 0.461 | 0.612 |
| 100% | 0.143 | 0.212 | 0.271 | 0.322 | 0.368 | 0.546 |
| 120% | 0.067 | 0.131 | 0.19 | 0.244 | 0.293 | 0.489 |
| 160% | 0.015 | 0.051 | 0.095 | 0.141 | 0.188 | 0.397 |
| 200% | 0.004 | 0.023 | 0.051 | 0.086 | 0.125 | 0.328 |
| 240% | 0.001 | 0.012 | 0.03 | 0.055 | 0.086 | 0.275 |
| 260% | 0.001 | 0.009 | 0.024 | 0.045 | 0.073 | 0.253 |
| 300% | 0 | 0.005 | 0.016 | 0.031 | 0.053 | 0.216 |